Incremental Redundancy - Hybrid Automatic Repeat Request Scheme in Next Generation Wi-Fi Systems

A Thesis

submitted by

SHISHIR G

in partial fulfilment of the requirements
for the award of the degree of

BACHELOR AND MASTER OF TECHNOLOGY

DEPARTMENT OF ELECTRICAL ENGINEERING
INDIAN INSTITUTE OF TECHNOLOGY MADRAS.

June 2020

THESIS CERTIFICATE

This is to certify that the thesis titled **Incremental Redundancy - Hybrid Automatic Repeat Request Scheme in Next Generation Wi-Fi Systems**, submitted by **Shishir G**, to the Indian Institute of Technology, Madras, for the award of the degree of **Bachelor and Master of Technology**, is a bona fide record of the research work done by him under our supervision. The contents of this thesis, in full or in parts, have not been submitted to any other Institute or University for the award of any degree or diploma.

Dr. David Koilpillai
Research Guide
Professor
Dept. of Electrical Engineering
IIT-Madras, 600036
Place: Chennai
Date: June, 2020

ACKNOWLEDGEMENTS

First and foremost, I express my sincere gratitude to my Research Guide, Prof. David Koilpillai, for his consistent guidance, motivation and support for my research work. I would also like to thank him for providing wonderful and unique opportunities for my growth. I have learned a lot from him as a researcher as well as a professional.

I would also like to thank my co-guide Prof. Nambi Seshadri for nurturing and advising. His incites on the problems have been a huge help in solving them. Our weekly meetings facilitated me in learning how to solve research problems. It was a pleasure working with him.

I thank Romil Sonigra and Ashutosh Nikam for their help in my research work. They have been a second pair of eyes throughout my DDP research.

I would like to thank my fellow researchers Sathwik Chadaga, Narendra Deconda, Major Sanjay Haojam and Major Arun Singh Pundir for creating an interesting, cheerful and proactive research environment. I will never forget the lab discussions and tea breaks.

I express my gratitude to my beloved parents Mr. H Ganesh Bhat, Mrs. Jayashree Bhat and my brother Shreesha Bhat for their constant support. At last I thank the Almighty and seek his divine blessings.

ABSTRACT

There has been rapid development in the next generation WiFi systems (IEEE 802.11ax and beyond). However, the lacuna in the WiFi systems has been the lack of optimized Automatic Retransmission (ARQ) protocols. The main reason for sticking to low-hanging fruits has been the attempt to minimize the complexity and buffering requirements in the user (STA) side. The task of maximizing the throughput while keeping the UE complexity at a minimum is a challenging and relevant one.

In this thesis, we explored the potential of using Hybrid ARQ (Incremetal Redundancy (IR) in particular) in the next generation WiFi systems (Extremely High Throughput (EHT) and later standards). We investigated how the Hybrid ARQ scheme combined with Adaptive Coding can improve the throughput by comparing it with the ARQ protocol that is currently defined in Wi-Fi standards. The effectiveness of IR-HARQ is mainly determined by the rate-compatible punctured codes, whose performance was also studied. From the simulation results presented, it can be observed that the Incremental Redundancy scheme provides around 3 dB gain when compared to ARQ protocol.

TABLE OF CONTENTS

LIST OF FIGURES

ABBREVIATIONS

WLAN	Wireless Local Area Network
LTE	Long Term Evolution
PSD	Power Spectral Density
SNR	Signal-to-Noise Ratio
PER	Packet Error Rate
BER	Bit Error Rate
ARQ	Automatic Repeat Request
HARQ	Hybrid Automatic Repeat Request
IR	Incremental Redundancy
PCC	Punctured Chase Combining
MCS	Modulation and Coding Scheme
AWGN	Additive White Gaussian Noise
FEC	Forward Error Correction
LDPC	Low-density Parity Codes
OFDM	Orthogonal Frequency Division Multiplexing
QAM	Quadrature Amplitude Modulation
STA	Station
LLR	Log-likelihood Ratio
k-SR	k Step Recoverable
CW	Contention Window
VoIP	Voice over Internet Protocol

CHAPTER 1

INTRODUCTION AND BACKGROUND OF THE TOPIC

Transmissions over wireless channels are subject to errors, due to variations in the received signal quality. To some degree, such variations can be countered through link adaptation. However, receiver noise and unpredictable interference variations cannot be countered. Therefore, all wireless communication systems employ Forward Error Correction (FEC), adding redundancy to the transmitted signal allowing the receiver to correct errors. In WLAN 802.11, Convolutional coding or LDPC coding (predominantly) is used for error correction.

Despite the error-correcting code, there will be data received in error, for example due to high noise or interference level. Hybrid Automatic Repeat Request (HARQ) tries to counter this issue by relying on a combination of error-correcting coding and retransmission of erroneous data. Data in error despite the error correcting coding are detected by the receiver, which requests a retransmission from the transmitter. Although it is in principle possible to attain a very low error probability with the hybrid-ARQ scheme, it comes at a cost in transmission resources such as power, the receiver resources like buffer and higher latency. One of the significant disadvantage of retransmission schemes in practice is that additional delays are introduced in the system. However in many practical systems, the number of retransmissions allowed is limited to avoid an unacceptable time delay before the successful transmission of a packet.

Currently in the Wi-Fi standards, the improvements in the throughput are obtained by adapting Modulation and Coding Scheme (MCS) based on the channel conditions through Channel Quality Information (CQI) feedback. Wi-Fi usage is increasing rapidly and hence there is a need for continuous improvements. Hybrid ARQ is a proven technology, which is being used in cellular (3G and 4G) and other unlicensed band wireless standards, that has the potential to give even better performance.

1.1 Different Retransmission Protocols

There are 3 retransmission schemes that are predominantly used in wireless communication.

- Automatic Repeat Request (ARQ)
- Chase Combining HARQ
- Incremental Redundancy HARQ

Retransmission Protocol	Description
ARQ	Receiver throws away the packet and asks for a retransmission
CC-HARQ	Receiver combines the similar versions of repeated bits from different transmissions
IR-HARQ	On request of a retransmission, the transmitter sends a different redundancy version of the parity bits

Table 1.1: Different retransmission protocols

1.1.1 Automatic Repeat Request (ARQ)

ARQ is an error-control method for data transmission that uses acknowledgements and timeouts to achieve reliable data transmission over an unreliable service. If the sender does not receive an acknowledgment before the timeout, it retransmits the packet until the sender receives an acknowledgment or exceeds a predefined number of retransmissions. The types of ARQ protocols include Stop-and-wait ARQ, Go-Back-N ARQ, and Selective Repeat/Reject ARQ. All the protocols use some form of sliding window protocol to tell the transmitter to determine which packets need to be retransmitted. In Stop-and-wait ARQ protocol, both the transmit and receive window sizes are equal to one, i.e, the sender sends one framer at a time. In Go-Back-N ARQ, the sliding window protocol has a transmit window size of N and receive window size of 1. The sender can transmit N frames before requiring an ACK. In Selective Repeat/Reject ARQ, the sender doesn't need to wait for individual ACK from the receiver. The receiver may selectively reject a single frame, which may be retransmitted alone. This contrasts with other forms of ARQ, which must send every frame from that point again.

They key difference of ARQ when compared to other retransmission protocols, is that it discards the log-likelihood ratio (LLR) information present in a failed transmission and only considers the LLR information of the new transmission. The advantage of this scheme is that the receiver need not store the LLR information of the failed transmissions which relaxes the buffer management. Whereas the obvious disadvantage is the fact that the decoder is missing out on some useful information from previous transmissions.

1.1.2 Chase Combining (CC-HARQ)

In the simplest version of HARQ, Chase Combining, every re-transmission contains the same information (data and parity bits). The receiver uses maximum-ratio combining (MRC) to combine the received bits with the same bits from previous transmissions. As all the transmissions are identical, Chase combining can be seen as additional repetition coding. It can also be viewed as increasing the Signal-to-noise ratio (SNR) of the transmission by M-fold (where M is the total number of transmissions).
The Shannon–Hartley theorem states the channel capacity,

$$C = log_2\left(1 + SNR\right) \tag{1.1}$$

As the repitition of same set of bits is equivalent to increase in SNR, the maximum achievable rate after M transmissions is given by [1]

$$C_{CC} = log_2\left(1 + \sum_{i=1}^{M} SNR_i\right) \tag{1.2}$$

where SNR_i is the SNR in the i^{th} transmission.

1.1.3 Incremental Redundancy (IR-HARQ)

In the Incremental Redundancy scheme, every re-transmission contains different information than the previous one. First transmission transmits a subset of the parity bits, the number decided based on the SNR conditions. The re-transmission uses a different set of coded bits than the previous transmission, with different redundancy versions generated by puncturing the encoder output. Thus, at every re-transmission the receiver gains extra information. These different versions are combined at the receiver while decoding.

As Incremental Redundancy scheme transmits different sets of bits in different transmissions, the maximum achievable rate after M transmissions is given by

$$C_{IR} = \sum_{i=1}^{M} log_2\left(1 + SNR_i\right) \tag{1.3}$$

where SNR_i is the SNR in the i^{th} transmission.

If we consider the difference in achievable rates between Incremental Redundancy and Chase Combining,

$$\begin{aligned}
\Delta C = C_{IR} - C_{CC} &= \sum_{i=1}^{M} log_2\left(1 + SNR_i\right) - log_2\left(1 + \sum_{i=1}^{M} SNR_i\right) \\
&= log_2\left[\frac{\left(1 + SNR_1\right)\left(1 + SNR_2\right)...\left(1 + SNR_M\right)}{1 + \sum_{i=1}^{M} SNR_i}\right] \\
&= log_2\left[\frac{1 + \sum_{i=1}^{M} SNR_i + \sum_{i,j=1}^{M} SNR_i SNR_j + ...}{1 + \sum_{i=1}^{M} SNR_i}\right] \\
\implies C_{IR} > C_{CC}
\end{aligned} \tag{1.4}$$

Thus it is shown that the maximum achievable rate with incremental redundancy scheme is greater than Chase Combining.

A slightly modified version of Incremental Redundancy is also considered in practice, where the data bits are repeated in every transmission, along with a new version of parity bits. The advantage of this scheme is that the packet is self-decodable, as each of its transmission contains the data bits. But the obvious disadvantage is the requirement of repitition of data bits.

CHAPTER 2

LITERATURE SURVEY

In this chapter we are going to discuss a survey on literature in Hybrid ARQ (HARQ) retransmission protocol. Initially, we will start with some early papers on HARQ and then we discuss some recent papers.

Hybrid Automatic Repeat Request (HARQ) was first proposed by Wozencraft and Horstein [2] in 1960. He showed that when the time-variant noisy two-way channels are protected by coding, they may be used to provide noiseless feedback, with delay, which can be utilised for performance improvement. In their celebrated work [3], Schalkwijk and Kailath showed that a simple linear feedback coding scheme achieves the capacity. They showed that the availability of the feedback link cannot increase the channel capacity of the noisy forward link, but it can considerably reduce the coding effort required to achieve a given level of performance. They showed that the associated probability of error decays doubly exponentially. Similarly, Lau [4], has shown that for Rayleigh fading channels with feedback, the associated error probability error decays dramatically when channel state is fed back to the transmitter and the associated Modulation and Coding Scheme is chosen that is matched to the channel state.

Hybrid ARQ has been extensively used in Cellular standards like 4G [5] [6]. As 4G uses turbo coding, the parity bits are represented in a circular buffer fashion and each redundancy version is defined by a different starting point in the buffer, starting from which the parity bits are chosen for transmission. The performance and complexity issues of having HARQ in LTE is studied in [7]. Shu Lin and Daniel Costello, in their book [8], anaylsed the thorughput efficiencies for different retransmission protocols. In the work carried out in [9], it was seen that Hybrid ARQ can provide a gain of around 2 dB on average in LTE. It also highlighted the fact that Hybrid ARQ schemes provide significant gain only at low and moderate Signal-to-noise ratio (SNR) conditions.

As the WLAN 802.11 standards predominantly use Low-density Parity Check (LDPC) codes for Forward error correction, it is important to understand the effect of puncturing in LDPC codes. One of the early works on LDPC puncturing for Incremental Redundancy HARQ was by Ramesh Mantha [10]. In this work, he analyses the performance of arbitrary uniform puncturing with masking and interleaver based rate-compatible puncturing. He aimed at ensuring that the transmitted parity bits are evenly spread throughput the LDPC parity-check matrix. In their work [11], Christopher Lott, Olgica Milenkovic and Emina Soljanin defined an IR-HARQ protocol where the parity bits are punctured from random locations to obtain a rate-compatible LDPC code. The obvious disadvantage of this protocol is the overhead invloved in communicating these locations to the receiver.

A path-breaking result was obtained in [12], where Jeongseok Ha and Jaehong Kim came up with a concept of k-Step Recoverable (k-SR) nodes for LDPC codes, where the value k is the number of LDPC iterations required to obtain a reliable log-likelihood information while decoding. The parity bits are categorised into 1-SR nodes, 2-SR nodes and so on. Based on this categorisation, the order of puncturing is determined.

In this thesis, we build upon previous works, and try to understand the impact Hybrid ARQ can have in WLAN 802.11 standards. The major focus is on obtaining the throughput curves with Incremental redundancy scheme and comparing it with the existing retransmission protocols in the standrads. Then we introduce certain constraints that needs to be satisfied in practice, and see the change in performance.

CHAPTER 3

SOLUTION APPROACH

IR-HARQ performance in WLAN 802.11 was analysed predominantly in four steps.

- Having a fixed set of code rates for different transmissions
- Deciding on the code rates based on the Long-term SNR
- Deciding on the code rates based on the Short-term SNR
- Considering the effect of mismatches and constraints

3.1 Fixed set of code rates for different transmissions

Initially, in Section 4.3, we analyse the performance of Incremental redundancy by fixing the set of code rates at which the transmissions happen. In the case of 4 transmission scheme, the code rates were fixed at $\{\frac{5}{6}, \frac{3}{4}, \frac{2}{3}, \frac{1}{2}\}$. Whereas, in the case of 2 transmission scheme, two sets of rates were considered, $\{\frac{2}{3}, \frac{1}{2}\}$ and $\{\frac{5}{6}, \frac{3}{4}\}$ and the one which gave the best throughput was selected. For a given modulation scheme, the first set would be chosen at low SNRs, whereas the second set would be optimal at high SNRs.

3.2 Deciding on the code rates based on Long-term SNR

Having a fixed set of rates, as defined in Section 3.1, is not an intelligent way of performing Incremental Redundancy, as it is fixing the rates to either a set or two, without taking into consideration the SNR. So in the next step, in Section 4.4, Long-term SNR information was used to make a decision on the code rates for different transmissions. For this, an SNR breakpoint model was designed. It defines the code rates at which the packets are to be sent, at different SNRs. At low SNRs, the code rates will be on the lower side, whereas at high SNRs, the rates will be high. As it was difficult to find the optimal set of rates at each and every SNR, we considered 4-5 different set of rates. The optimal one among these set of rates were obtained, at each SNR.

3.3 Deciding on the code rates based on Short-term SNR

Using Long-term SNR as the decision metric, as defined in Section 3.2, is not the optimal way of deciding on code rates. This is because of the time-varying nature of SNR due to fading experienced in the channel. So in the next step, in Section 4.5, Short-term SNR information was used to make a decision on the code rates for different transmissions. As this requires an estimate of instantaneous SNR of the next packet, Auto-regressive model was used to predict the SNR, as the autocorrelation (given by Bell Spectrum model in WLAN 802.11) is known to us.

3.4 Including the effect of mismatches and constraints

Assumption of the perfect SNR knowledge is not realistic. So in Subsection 4.5.3, the SNR was assumed to be uniformly distributed around the actual SNR and the performance was analysed based on this mismatch.

As it is important to have a reasonable Packet Error Rate (PER) that can be handled by higher layers, in Section 4.6, a constraint was imposed on the final transmission that the PER should be smaller than a certain value.

In real-time applications like VoIP calls and YouTube streaming, retransmissions can't happen beyond a certain delay, after which the packet will have to be discarded. This issue of latency is analysed in Section 4.7

CHAPTER 4

PERFORMANCE SIMULATIONS AND KEY RESULTS

4.1 Basic Simulations

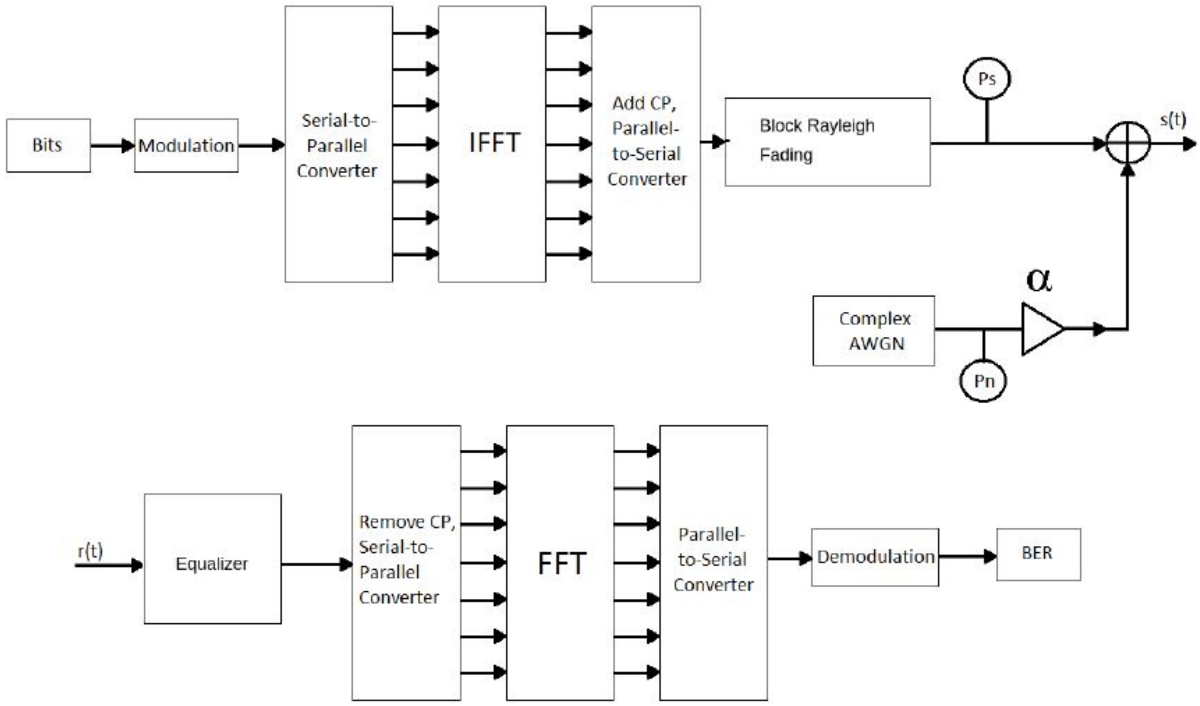

Figure 4.1: Block Diagram for Simulation of BER performance in an OFDM system in a Rayleigh Fading channel

Some basic simulations were performed in AWGN and Rayleigh fading channel. The block diagram for these simulations is shown in Figure 4.1.

Figures 4.2 and 4.3 show the BER performance without FEC for different modulation schemes in AWGN channel and Rayleigh fading channel respectively. As expected, in AWGN case, the BER falls off like a waterfall, whereas with Rayleigh fading the BER fall is linear in log scale.

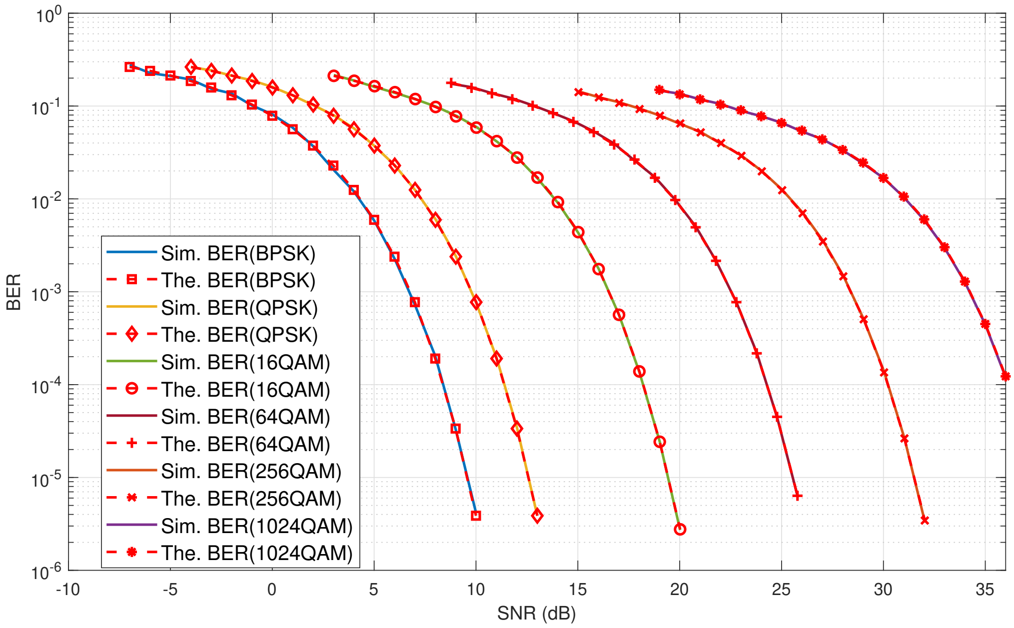

Figure 4.2: AWGN BER Performance in an OFDM system without FEC

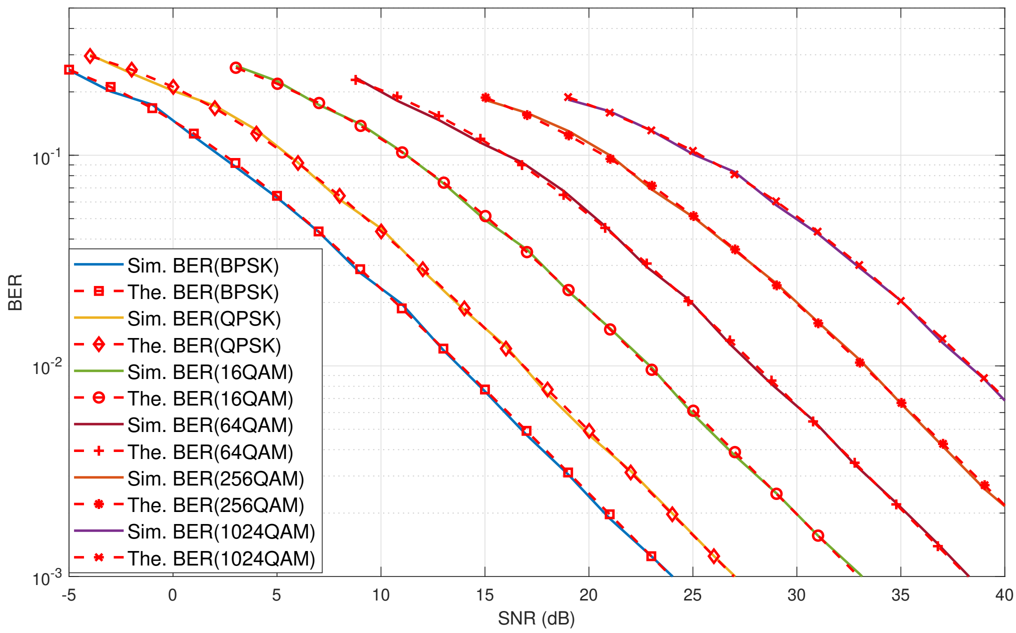

Figure 4.3: Rayleigh Fading BER Performance in an OFDM system without FEC

4.2 Performance of LDPC Codes defined in WLAN standards

802.11ax standard defines 12 different Modulation and Coding Schemes (MCS) (Table 4.1)

MCS index	Modulation Type	Coding Rate
0	BPSK	$\frac{1}{2}$
1	QPSK	$\frac{1}{2}$
2	QPSK	$\frac{3}{4}$
3	16QAM	$\frac{1}{2}$
4	16QAM	$\frac{3}{4}$
5	64QAM	$\frac{2}{3}$
6	64QAM	$\frac{3}{4}$
7	64QAM	$\frac{5}{6}$
8	256QAM	$\frac{3}{4}$
9	256QAM	$\frac{5}{6}$
10	1024QAM	$\frac{3}{4}$
11	1024QAM	$\frac{5}{6}$

Table 4.1: MCS in WLAN 802.11ax standard

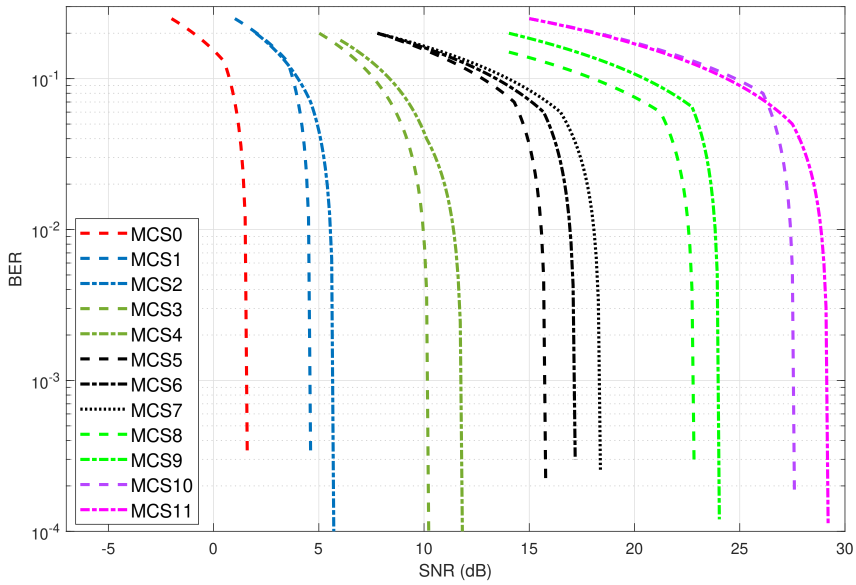

Figure 4.4: WLAN 802.11 LDPC BER Performance

Figure 4.4 shows the LDPC BER performance for different MCS defined in the Table 4.1 .

Figure 4.5 compares the performance of LDPC codes for different codeword lengths. LDPC with codeword length of 1944 bits has an SNR gain of around 0.5 dB and 0.8 dB when compared

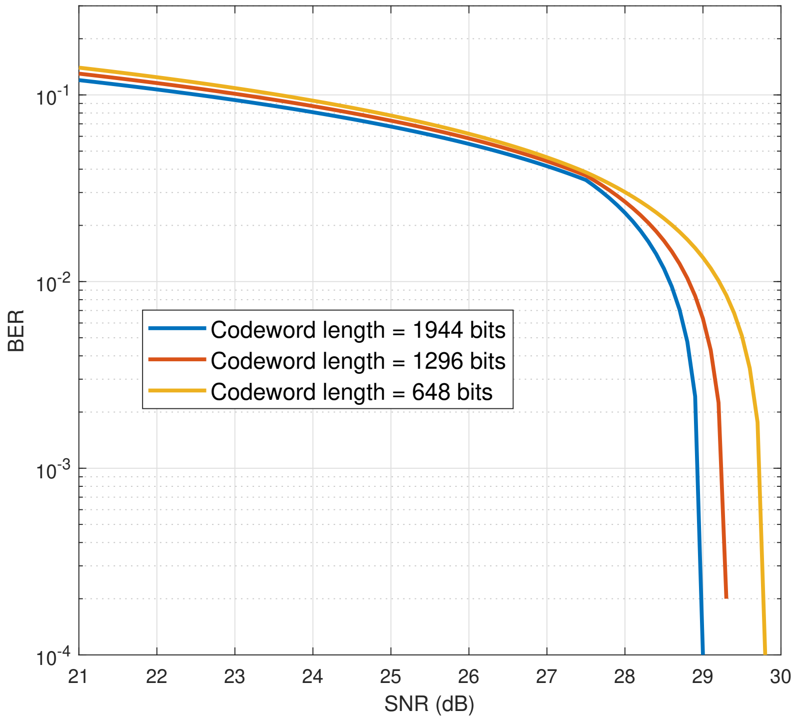

Figure 4.5: Comparison of LDPC BER Performance with different Codeword lengths

to codeword lengths of 1296 bits and 648 bits respectively.

4.3 IR-HARQ scheme based on fixed set of Rates

The WLAN 802.11 standard [13] defines LDPC mother codes of 4 different rates $\{\frac{5}{6}, \frac{3}{4}, \frac{2}{3}, \frac{1}{2}\}$. The performance of Incremental Redundancy was analysed fixing the rates at these values. In the case of 4 transmissions, a rate-$\frac{1}{2}$ mother code is punctured to get rate-$\frac{5}{6}$, rate-$\frac{3}{4}$ and rate-$\frac{2}{3}$ codes. In the case of 2 transmissions, 2 schemes were considered. Puncturing a rate-$\frac{1}{2}$ mother code to obtain a rate-$\frac{2}{3}$ code and puncturing a rate-$\frac{3}{4}$ mother code to obtain a rate-$\frac{5}{6}$ code. The best among these two schemes were considered at a given SNR.

4.3.1 Simulation Setup

- Channel Model: WLAN tgax Model-D [14]
- Correlation Model: Bell Spectrum (Figure 4.7(a))
- Packet size: 1 kByte

- Doppler, $f_d = 5$ Hz

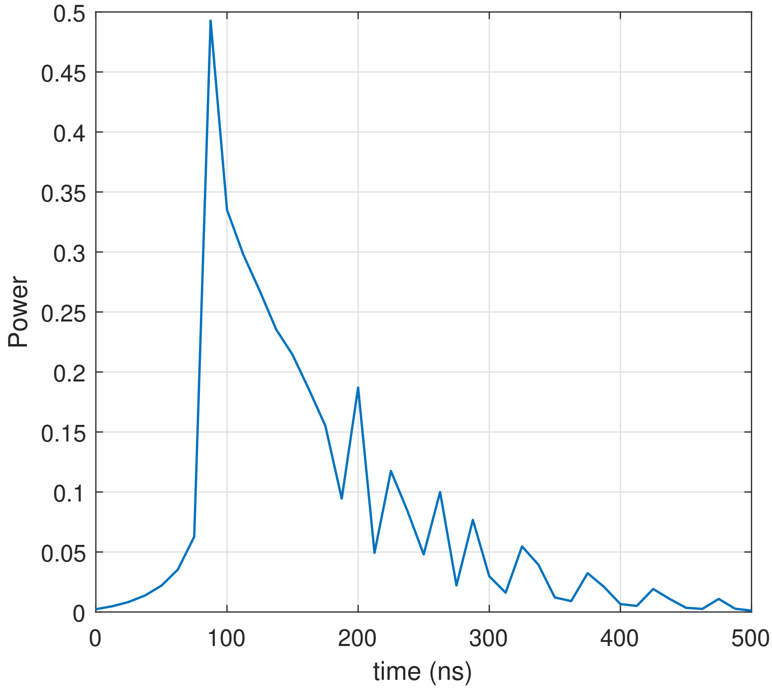

Figure 4.6: Power Delay Profile of WLAN TGax Channel Model-D

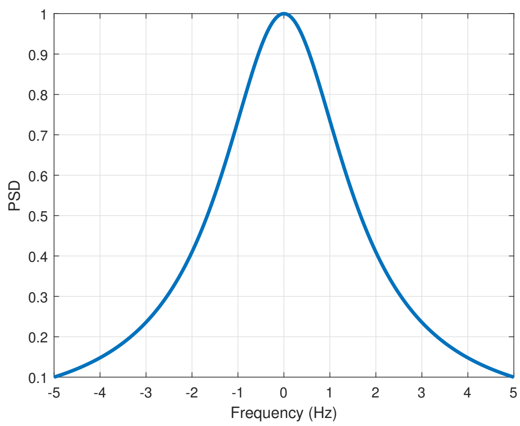

(a) Bell Spectrum (WLAN)

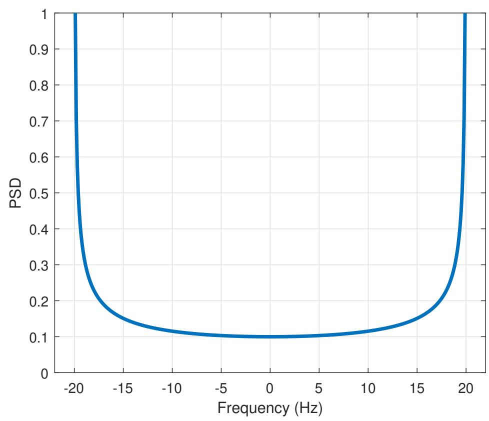

(b) Jakes Spectrum (LTE)

Figure 4.7: Comparison of Correlation Spectrum in WLAN and LTE standards

Figure 4.8 has the PER and throughput plots for 64QAM modulation. Similar curves were obtained for other modulation schemes.

Figure 4.9 shows the throughput curves when the number of transmissions allowed are varied. It can be observed that there is a significant gain in moving from just a single transmission to allowing for 2 transmissions, but the gain diminishes when we allow for 4 transmissions.

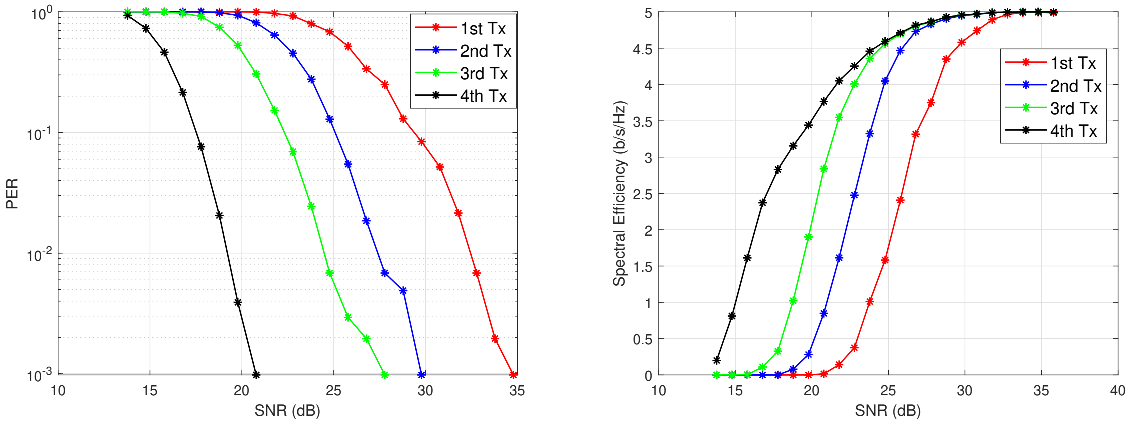

(a) PER (b) Throughput

Figure 4.8: PER and Throughput Plots for IR-HARQ fixed-rate scheme (64QAM)

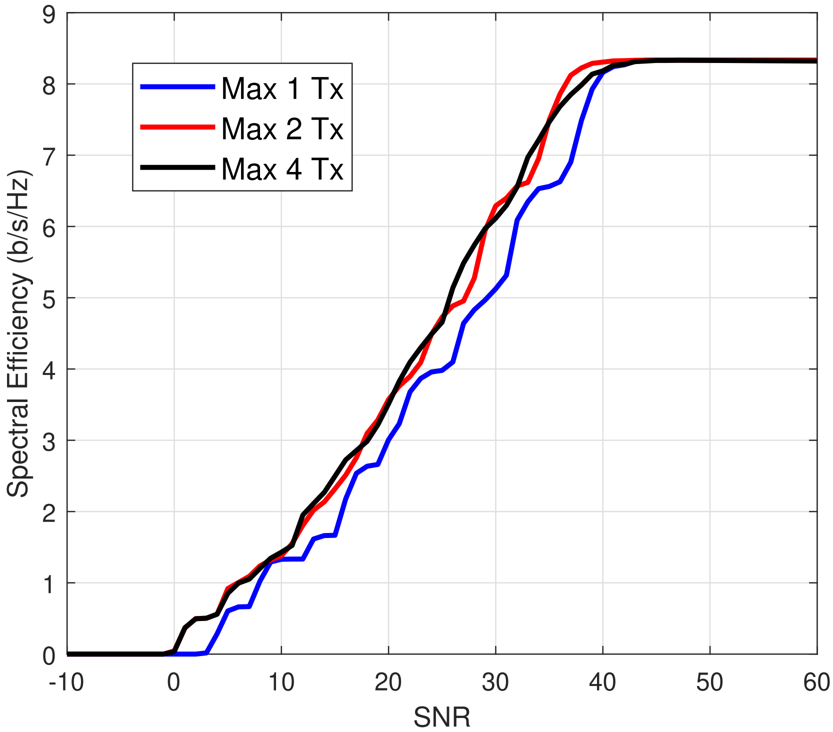

Figure 4.9: IR-HARQ performance with different number of transmissions (Fixed-rate scheme)

This is the shortcoming of the K-Step Recoverable (k-SR) puncturing technique that is being considered here for LDPC codes (Refer Appendix 7.3).

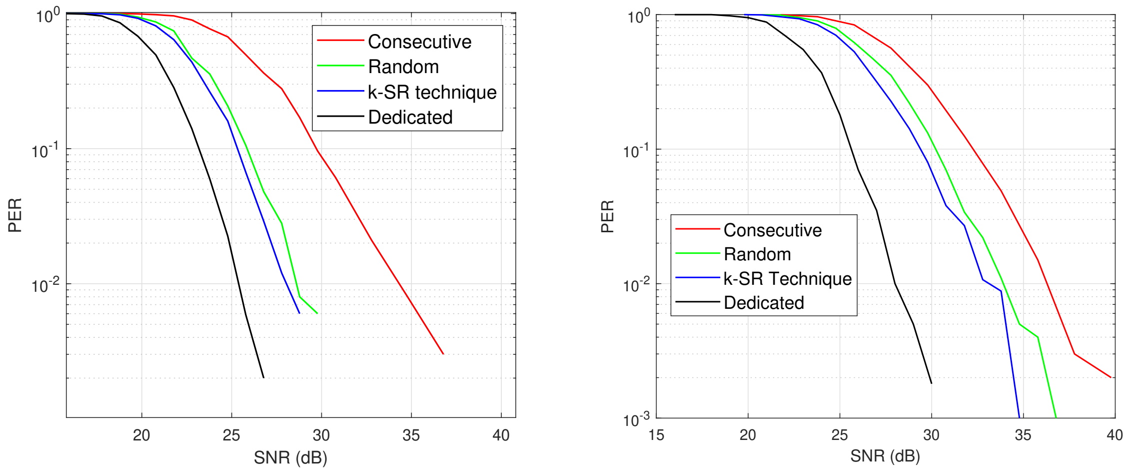

(a) Rate-$\frac{3}{4}$ Code (b) Rate-$\frac{5}{6}$ Code

Figure 4.10: Effect of Puncturing in LDPC Codes

In the Figure 4.10, the performance of different puncturing techniques have been compared with the dedicated-code performance. In the Consecutive technique, contiguous set of parity bits are punctured. In the Random technique, parity bits are punctured from random locations. It can be observed that the performance of a rate-$\frac{3}{4}$ code obtained by puncturing a rate-$\frac{1}{2}$ mother code is poorer by 2.5 dB when compared to a dedicated rate-$\frac{3}{4}$ code. This gap widens to around 4 dB when we consider a punctured rate-$\frac{5}{6}$ code. In the case of 2 transmissions, the mother code needs to be punctured only to its next higher rate, because of which the effect of puncturing isn't visible. Whereas with 4 transmissions, a rate-$\frac{1}{2}$ mother code is punctured to obtain a rate-$\frac{5}{6}$, taking a hit on performance as seen in Figure 4.9 .

In Figure 4.11, it can be observed that in the case of 2 transmissions, IR-HARQ performance is better than ARQ and PCC as expected. But with 4 transmissions, IR-HARQ performance is only marginally better than PCC-HARQ because of the puncturing issue as seen in the Figure 4.10.

The comparison of different protocols with fixed-rate scheme has been quantified in the Table 4.2 .

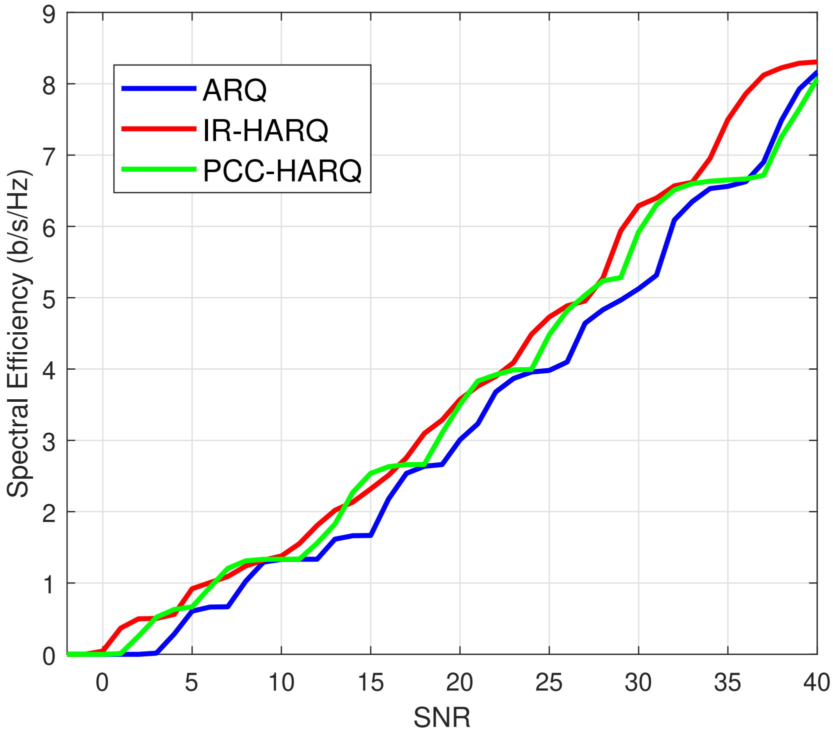

(a) 2 transmissions

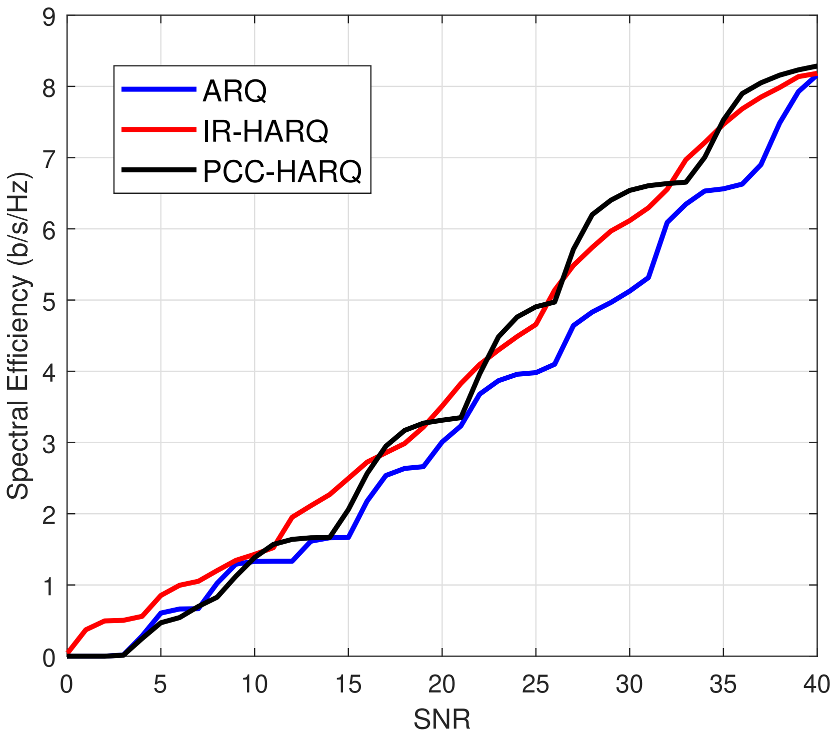

(b) 4 transmissions

Figure 4.11: Performance Comparison of IR vs PCC vs ARQ for fixed rate scheme

Comparison between	SNR Gain
IR-HARQ vs ARQ (2 Tx)	2.42 dB
IR-HARQ vs ARQ (4 Tx)	2.58 dB
IR-HARQ vs PCC-HARQ (2 Tx)	1.1 dB
IR-HARQ vs PCC-HARQ (4 Tx)	0.33 dB

Table 4.2: SNR gain comparison between different schemes for fixed-rate strategy

4.4 IR-HARQ scheme based on Long-term SNR

In the previous sections, the rates were fixed for all the transmissions, irrespective of the SNR. It was $\{\frac{5}{6}, \frac{3}{4}, \frac{2}{3}, \frac{1}{2}\}$ for 4-transmission scheme and two sets of $\{\frac{5}{6}, \frac{3}{4}\}$ and $\{\frac{2}{3}, \frac{1}{2}\}$ for 2-transmission scheme. This is nowhere near the optimal scheme, as it is not using the information about SNR, based on which decisions can be made. If the Long-term SNR is high, the rates can be chosen aggressively, whereas if the SNR is bad, the rates have to be chosen conservatively.

4.4.1 SNR Breakpoint Model

Ideally, one would consider a very low-rate code at low SNRs and gradually increase the rates with increasing SNR. As it is difficult to come up with optimal rates at each SNR, a breakpoint model was created, where 4-5 different sets of rates were considered for different SNR regions as shown in the Figure 4.12

At low SNRs, in the case of 4 transmissions, the packet is initially transmitted with rate $\frac{2}{3}$ and in the final transmission, the rate falls to $\frac{1}{4}$, whereas for 3-transmission scheme, the starting rate is slightly lower at 0.6 and in the final transmission it falls to 0.32.
At high SNRs, in the case of 4 transmissions, the packet is initially transmitted with an aggressive rate of 0.9 and in the final transmission, the rate falls to 0.42, whereas for 3-transmission scheme, the rate varies from 0.9 to 0.6. There are 3 breakpoints in our model, where the rates change.
The breakpoints and the corresponding rates were obtained based on the ARQ throughput curves. For a given SNR, ARQ has the best throughput for a specific set of rates $\{R, \frac{R}{2}, \frac{R}{3}, ...\}$. IR-HARQ rates and breakpoints are chosen in a slightly aggressive fashion based on this information. The rates can also be decided based on a certain Packet Error Rate (PER) constraint that needs to be satisfied after the last transmission. We will come to the effect of having PER

constraints later in section 4.6.

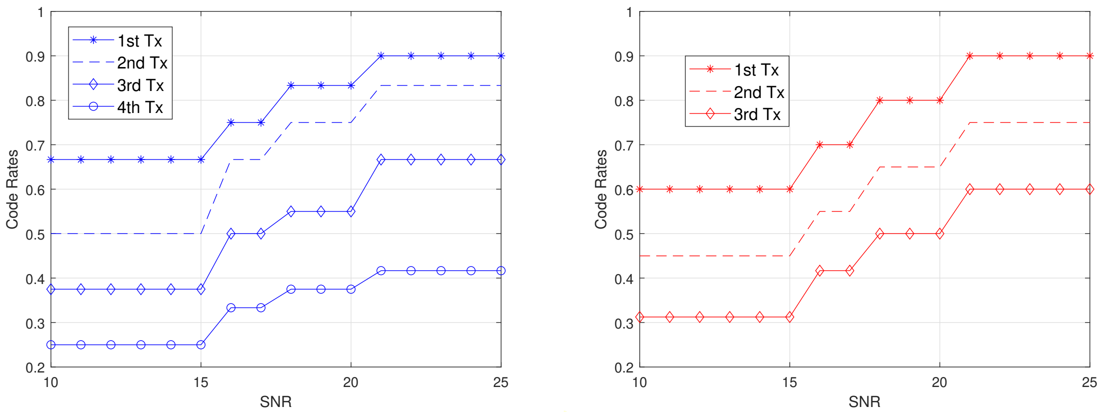

(a) 4 transmissions (b) 3 transmissions

Figure 4.12: SNR Breakpoint Model: Rates vs SNR (64QAM)

4.4.2 Simulation Results

Incremental Redundancy scheme was simulated considering the SNR breakpoint model described above. The throughput plot (maximum 4 transmissions allowed) is shown in Figure 4.13. Similar plots were obtained when the transmissions are restricted to 2 and 3.

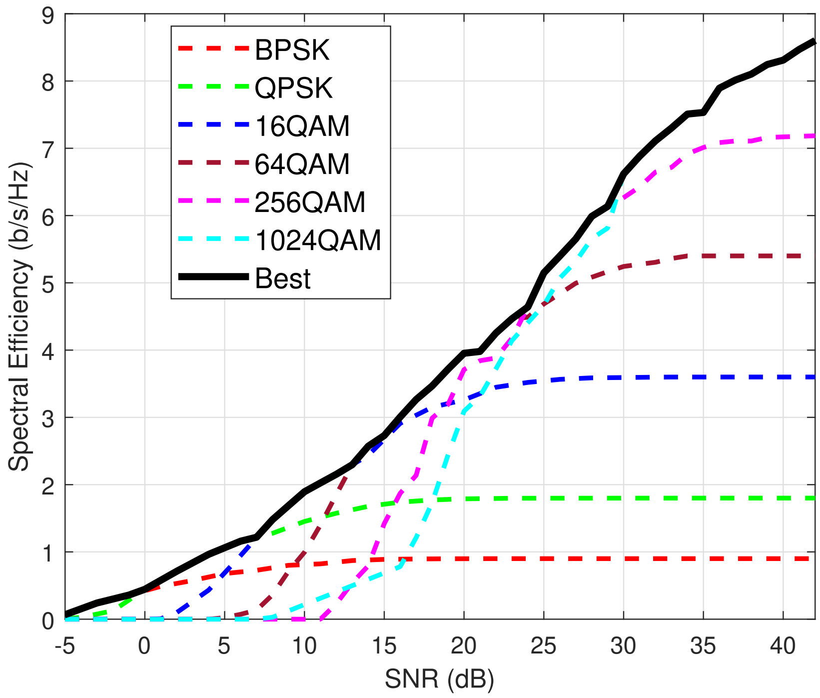

Figure 4.13: IR-HARQ throughput (4 transmissions) with Long-term SNR decision metric

Figure 4.14 compares the IR-HARQ throughput as the number of transmissions are varied. Figure 4.15 compares the throughput of IR-HARQ vs PCC vs ARQ when 4 transmissions are allowed.

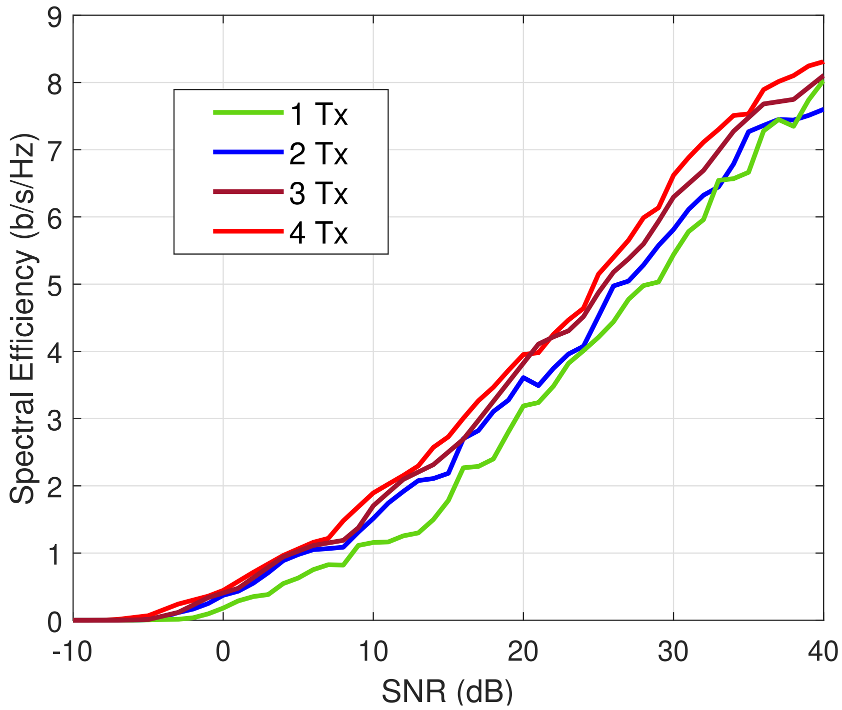

Figure 4.14: Comparison of IR-HARQ throughput with different number of transmissions (Long-term SNR decision metric)

The comparison between different schemes in the form of SNR gain has been quantified in Table 4.3.

Comparison between	SNR Gain
IR-HARQ vs ARQ	2.47 dB
IR-HARQ vs PCC-HARQ	0.03 dB
IR-HARQ (4 Tx) vs IR-HARQ (1 Tx)	3.79 dB
IR-HARQ (4 Tx) vs IR-HARQ (2 Tx)	2.49 dB
IR-HARQ (2 Tx) vs IR-HARQ (1 Tx)	1.41 dB

Table 4.3: SNR gain comparison between different schemes for Long-term SNR based strategy

It can be observed that IR-HARQ is the clear winner when compared to ARQ protocol that is being followed in the current WLAN standard. IR-HARQ is also expected to perform slightly better than PCC-HARQ. But in our simulations, IR-HARQ is performing better only by the slightest of margins. This is because of the performance degradation due to puncturing (Figure 4.10) which affects IR-HARQ, but not PCC-HARQ.

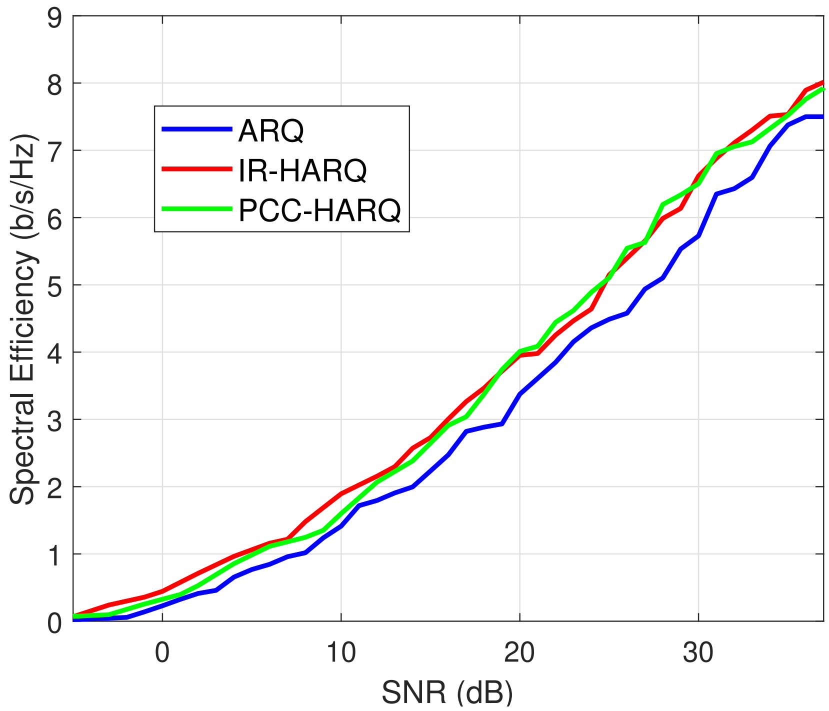

Figure 4.15: IR-HARQ vs PCC-HARQ vs ARQ throughput (Long-term SNR decision metric)

And as we move from 1-transmission scheme to 2-transmission scheme, the gain is significant, whereas the gain is diminishing as we further increase the number of transmissions allowed. Thus, having more than 4 transmissions doesn't add much value, as it results in a significant increase in latency, with a marginal increase in throughput.

4.5 Short-term SNR based Rate decision

Until now, we have been considering Long-term SNRs to make a decison on what rates to send the packets at, using the SNR breakpoint model. As we are considering a time-varying Rayleigh fading channel model, the Short-term (instantaneous) SNR will be varying around the Average SNR. So it is expected that the decison made based on Short-term SNR will perform better than the one made based on Long-term SNR.

4.5.1 Theoretical Analysis

For now, we are assuming that the receiver estimates the SNR perfectly and feeds it back to the transmitter. Given the instantaneous SNR of the previous packet, we estimated the SNR that the next packet experiences, and decide on what rates to use based on this estimated SNR value.

PSD of Bell spectrum correlation model is given as follows (Figure 4.7(a))

$$S(f) = \frac{1}{1 + 9\left(\frac{f}{f_d}\right)^2} \quad |f| \leq f_d \tag{4.1}$$

Corresponding autocorrelation is given as follows

$$R_h(\Delta t) = \frac{\pi f_d}{3} exp\left(-\frac{2\pi}{3} f_d \Delta t\right) \tag{4.2}$$

with a coherence time of $T_c = \frac{1.04}{\pi f_d}$.

Auto-regressive model on instantaneous SNRs is formulated as follows

$$SNR_t = \sum_{i=1}^{M} a_i SNR_{t-i} + c + \epsilon_t \tag{4.3}$$

where, SNR at time instant t is assumed to be a linear combination of SNRs at time instant $\{t - M, t - (M - 1), ..., t - 2, t - 1\}$ with an error term of ϵ_t and a term c to match the means of the left hand side and the right hand side.
There is a direct correspondence between these parameters a_i and the covariance function of the process. It can be shown that the autocorrelation is related as follows

$$R_t = \sum_{i=1}^{M} a_i R_{t-i} + noise \tag{4.4}$$

We already know the autocorrelation values from equation 4.2. These set of linear equations are solved to find the coefficients a_i's. Given these coefficients, the SNR for the next packet is estimated using equation 4.3. As the rates for all n transmissions have to be decided at the first transmission of the packet, a single SNR has to be deduced to make the decision, from n estimated SNRs. For this, next packet is assumed to have the same number of transmissions as the previous packet, and the SNR is estimated for the central transmission.
The comparison of True SNR vs Estimated SNR is shown in Figure 4.16 for $M = 2$ and $M = 4$.

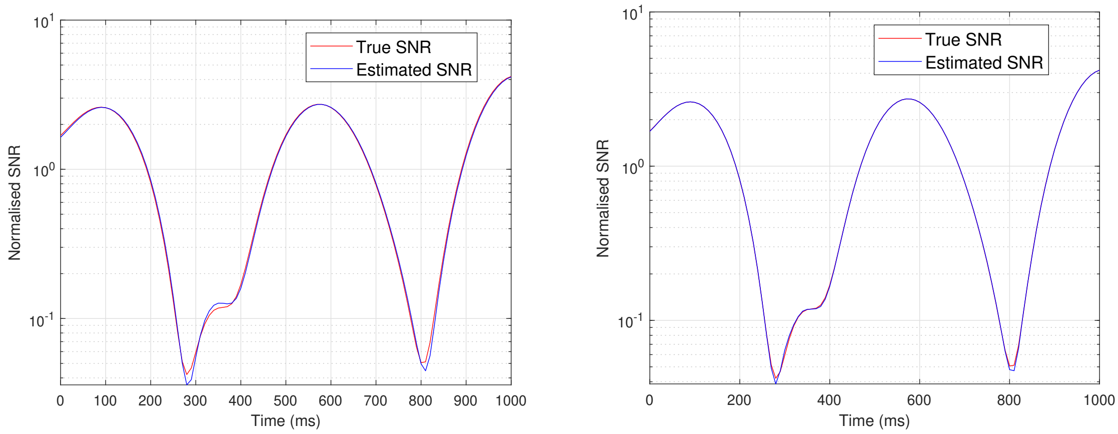

(a) $M = 2$

(b) $M = 4$

Figure 4.16: Estimated SNR vs True SNR using Auto-regressive model

Considering just two previous SNR values, the model gives a reasonable estimate of the future SNR, whereas if we keep increasing M, the estimate become more and more accurate.

4.5.2 Simulation results

Simulation parameters: $f_d = 5Hz$, Transmissions are assumed to happen at an interval of 10ms. So we sampled the autocorrelation at 100Hz and applied the Auto-regressive model to estimate future SNRs.

(a) Maximum 2 transmissions

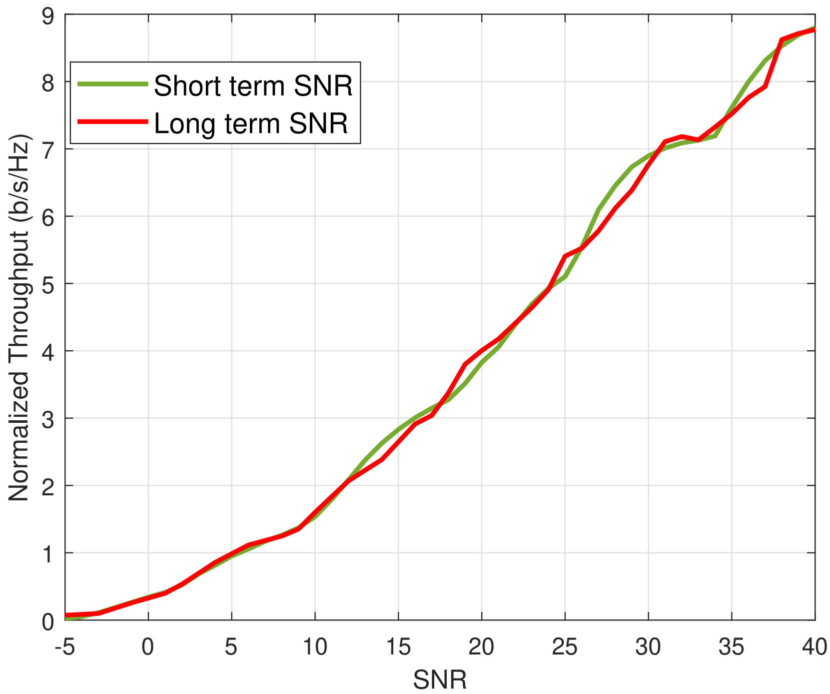

(b) Maximum 4 transmissions

Figure 4.17: IR-HARQ Throughput comparisons with Long-term SNR vs Short-term SNR based decisions

When the number of transmissions are restricted to 2 as shown in Figure 4.17(a), there seems to be a significant benefit throughout the SNR range, in using Short-term SNR (ST-SNR) feedback for making decisions. It has an average SNR gain of 1.3 dB when compared to Long-term SNR (LT-SNR) based scheme. This is expected, as the 2 transmissions won't be able to cover a wide range of rates, because of which the decision won't be optimal when the instantaneous SNR is far from LT-SNR.
When the number of transmissions are restricted to 4 as shown in Figure 4.17(b), ST-SNR scheme is only marginally better than LT-SNR scheme. As the 4 transmissions are anyway covering a wide range of rates, using ST-SNR feedback is not of high value in making decisions.

4.5.3 Effect of SNR Mismatch on IR-HARQ throughput

In the previous parts, it was being assumed that the receiver estimates the SNR perfectly and feeds it back to the transmitter which makes a decision on the transmission rates for the next packet based on this information. In practice, it is impossible for the receiver to perfectly estimate the SNR and the feedback that is sent back to the transmitter will also be quantized. Thus, it is important to understand the effects of these imperfections.
To model this mismatch, instead of making the decision based on the exact SNR, the decision is made on an SNR that is randmoly picked from a region surrounding the exact SNR. For this, a random variable picked from a Uniform distribution $[-\Delta, \Delta]$ dB is added to the exact SNR, and this new SNR is used to decide on the Rates with the help of SNR breakpoint model discussed in the subsection 4.4.1 .

From the Figure 4.18, it can be observed that without any mismatch, the instantaneous SNR varies $[-5, 5]$ dB around the average SNR, whereas with the mismatch, the distribution spreads out more as expected, which will lead to performance degradation.

Figure 4.19 shows the comparison of Incremental Redundancy throughput performance with and without SNR mismatch. Assumption of no SNR mismatch has an SNR gain of 0.54 dB over $[-3, 3]$ dB mismatch and 1.18 dB gain over $[-5, 5]$ dB mismatch.

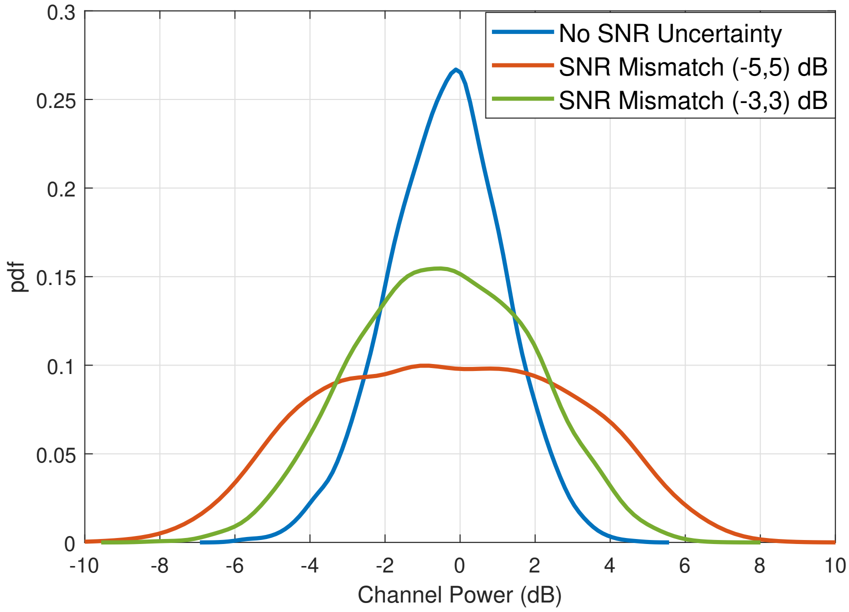

Figure 4.18: SNR distribution with and without SNR mismatch

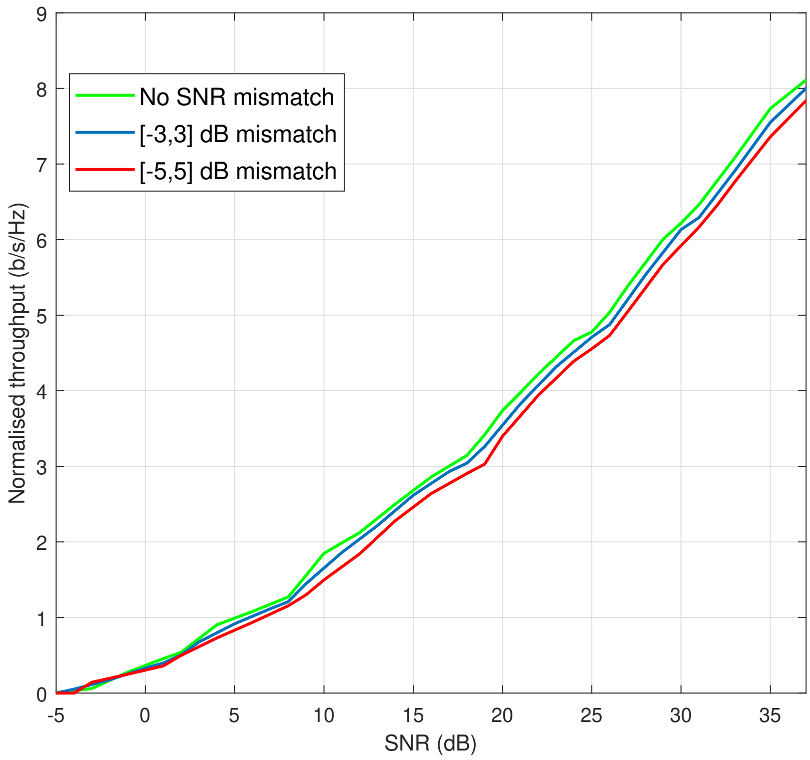

Figure 4.19: IR-HARQ throughput comparison with and without SNR mismatch

4.6 Effect of PER constraints on IR-HARQ throughput

Until now, the throughputs were being simulated without taking into consideration the Packet Error Rate (PER) performance. As it is important to have a reasonable PER, that can be handled by higher layers, PER constraints were put on the last transmissions. Say at a certain SNR, 64 QAM scheme gives the best throughput. If it doesn't satisfy the PER constraint, then 16 QAM scheme (which will have a lower PER at the same SNR) will be considered.

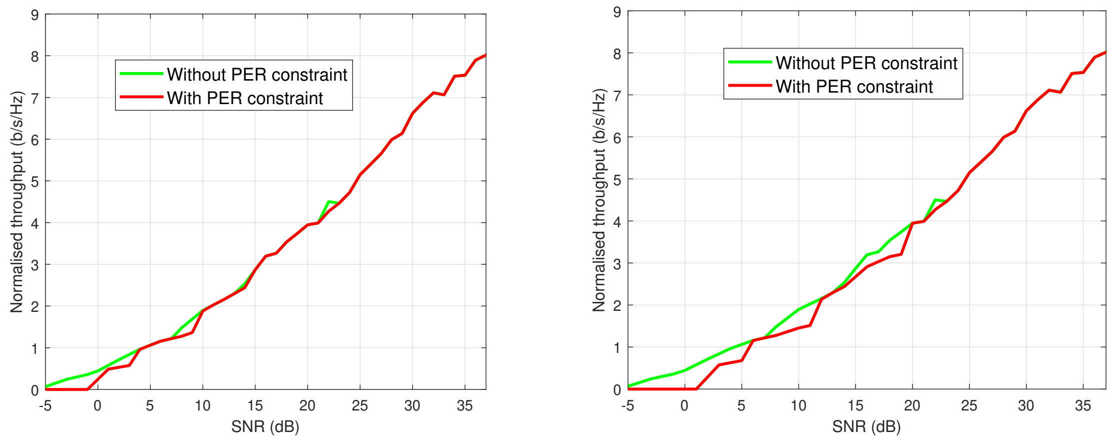

(a) PER constraint = 10^{-2}

(b) PER constraint = 10^{-3}

Figure 4.20: IR-HARQ throughput with different PER constraints (4 transmissions)

Figure 4.20 compares the IR-HARQ throughputs with and without PER constraints. It can be observed that a conservative constraint of 10^{-2} doesn't alter the throughput by much, whereas an aggressive constraint of 10^{-3} will result in a significant degradation.

Figure 4.21 compares IR-HARQ throughputs with and without PER constraints as the number of transmissions are varied. With 4 transmissions, having the PER constraint doesn't make much difference whereas if the transmissions are restricted to 2, there is a significant dip in the throughput. As the 4-transmission scheme can transmit packets at rates as low as $\frac{1}{4}$, the PER will be reasonable, whereas 2 transmissions will not be covering a wide range of rates, because of which PER constraint might not always be satisfied with the modulation scheme that gives the best throughput. The comparisons are quantified in Table 4.4.

With stronger constraints, the rates need to be chosen conservatively. The results obtained above, considered a single breakpoint model irrespective of the constraint. Ideally, as shown in Figure 4.22, the rate curves have to be shifted towards right as the constraint gets more aggressive.

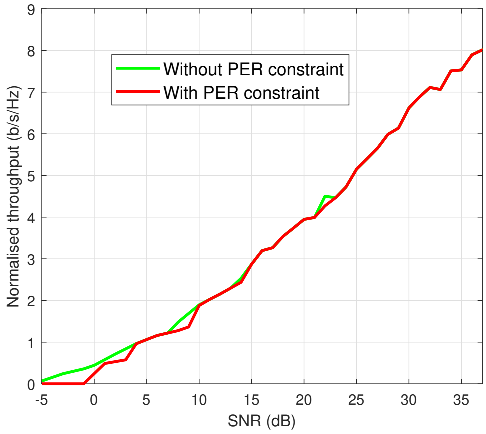

(a) Maximum 4 transmissions

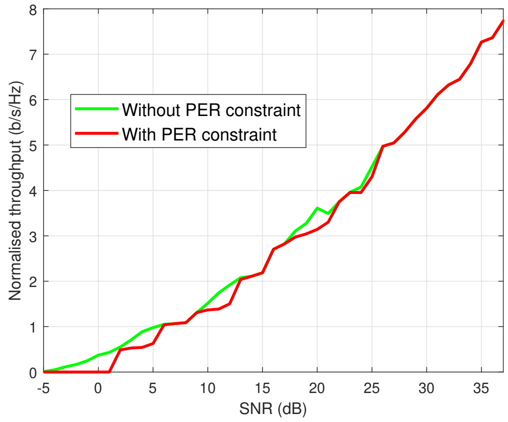

(b) Maximum 2 transmissions

Figure 4.21: IR-HARQ throughput with different number of transmissions (Constraint = 10^{-2})

Comparison with and without PER constraint	SNR Gain
4 transmissions, PER=10^{-2}	0.22 dB
4 transmissions, PER=10^{-3}	0.81 dB
2 transmissions, PER=10^{-2}	0.51 dB

Table 4.4: SNR gain comparison with and without PER constraints

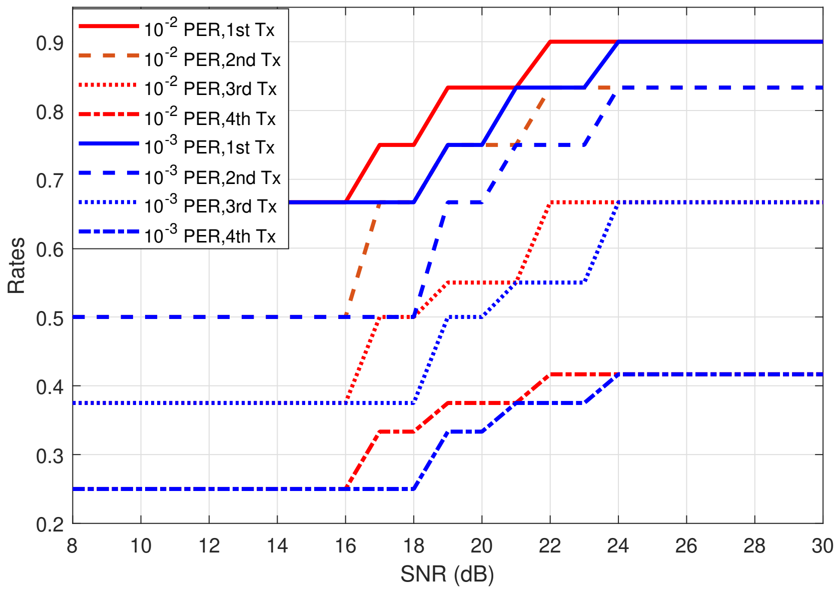

Figure 4.22: SNR breakpoint model with varying PER constraints

4.7 Effect of Latency constraints on IR-HARQ throughput

Until now, we have been simulating the throughput without considering the factor of latency involved in transmission. More the number of transmissions, higher the delay involved, which involves multiple contention periods.
If we consider the applications like Voice/Video calls and YouTube streaming, latency is an important factor. The receiver cannot keep waiting for the packet as they are real-time applications. In such scenarios, the maximum number of transmissions allowed must be fixed keeping in the mind the latency constraint. As the delay involved is proportional to the active number of STAs, we analysed the throughput with varying number of STAs. The average packet delay vs number of STAs was analysed, from which the decision can be made on how many transmissions to allow.

4.7.1 Simulation results

- Slot time, $\sigma = 9\ \mu s$
- Minimum Contention window length: 16
- Maximum Contention window length: 1024

As the different applications have different latency constraints, we considered a hypothetical scenario where all the active STAs are on VoIP calls. The end-to-end latency constraint is around 100-150 ms. We considered a delay constraint of 30 ms in Physical layer.

The expressions for collision probability and average packet latency have been derived in the appendix 7.4.

As the number of collisions increase with number of STAs (Figure 4.23), the latency is expected to increase with an increasing slope. But in the Figure 4.24, the latency increases linearly. This is the drawback of an assumption. In the analysis, we assumed that all the STAs are active always, i.e, the STAs will keep contending for resources throughout. But this is not the case in practice because the STAs keep quiet after they get to transmit until its buffer is filled again. Time taken to fill the buffer will be higher when the number of STAs are very low as the STAs get channel access more often. Thus, the assumption we made overestimates the latency. Actual latency curve will be below the one in Figure 4.24 and the difference will be higher on

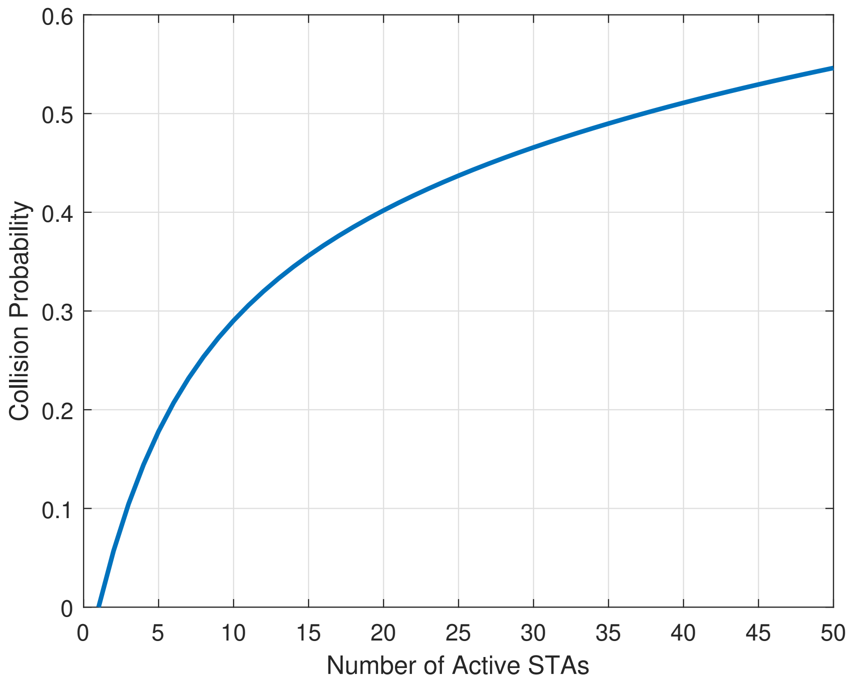

Figure 4.23: Collision Probability vs Number of STAs

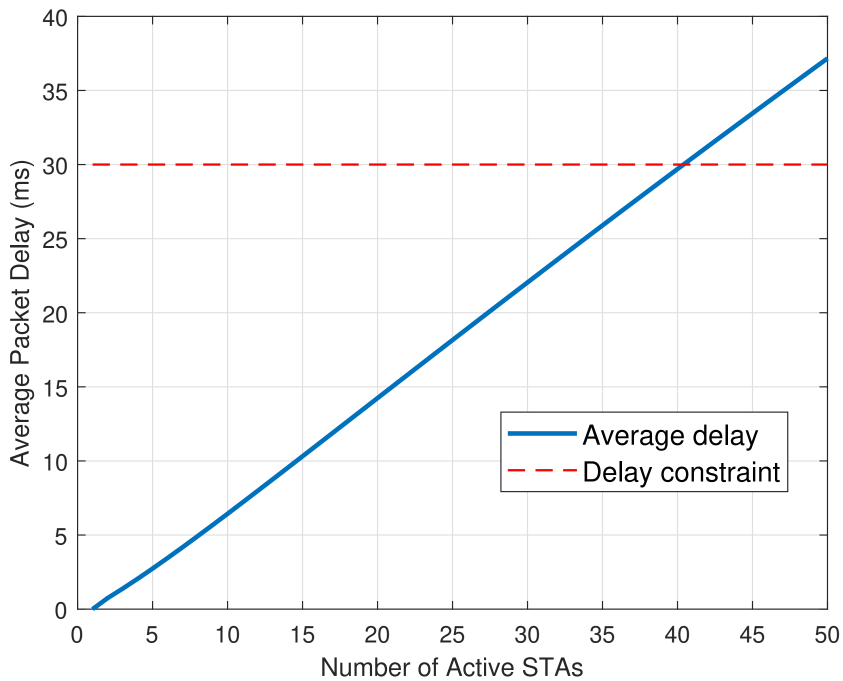

Figure 4.24: Average Packet Latency vs Number of STAs

the left hand side of the curve where there are very few STAs. Thus the actual latency curve, will have an increasing slope.

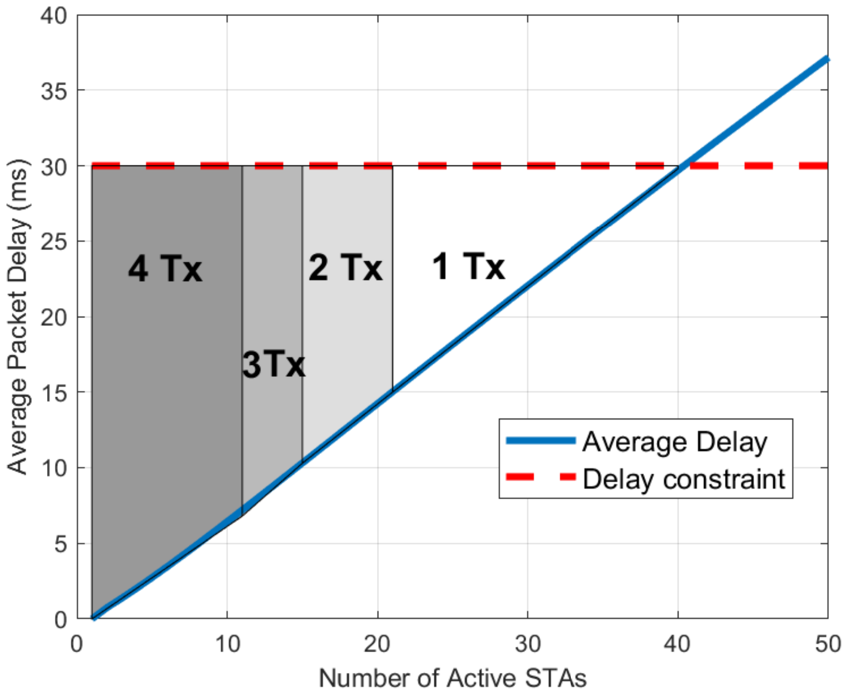

Figure 4.25: Maximum transmissions allowed vs Number of STAs

From the Figure 4.25 it can be seen that the maximum number of transmissions have to be set based on the number of active STAs. Upto 12 STAs, the collisions are low and upto 4 transmissions can be supported, whereas if there are around 25 or more STAs, only one transmission can be supported.

As more number of transmissions are allowed with lesser number of active STAs, the per Station Throughput reduces with increasing STAs, as show in Figure 4.26. This dynamic way of choosing the number of transmissions, based on the number of active STAs, gives a 7% increase in throughput as compared to fixing the scheme at two transmissions irrespective of the number of STAs.

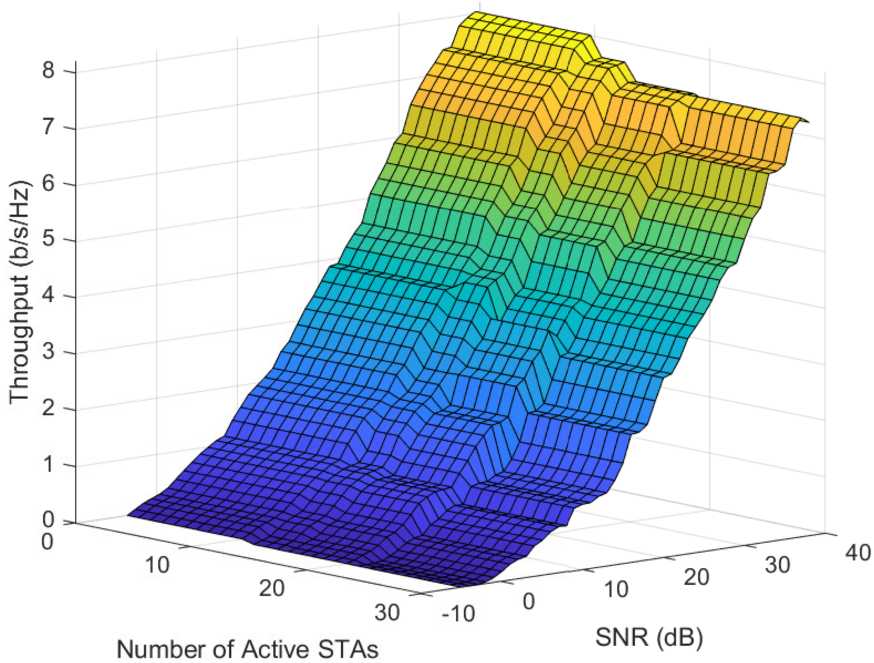

Figure 4.26: Throughput and Delay performance with SNR

CHAPTER 5

FUTURE WORK

There are a lot of avenues to explore continuing this work on HARQ. Some of the areas that can be explored are as follows.

- Explore other **puncturing techniques** for LDPC codes and try to reduce the performance gap between the punctured LDPC code and the dedicated code, that will benefit the Incremental Reduncdancy HARQ.
- Analyse the benefits of Incremental Redundancy with **MIMO**, as most of the wireless communication today happens with multiple antennas.
- **Buffer management** with Incremental Redundancy needs to be analysed as the chip area occupied by the HARQ buffer is becoming increasingly significant [15]
- Anaylse the effect of **LLR quantization** on Incremental Reduncdancy performance, as the simulations here considered very high precision.
- Study the effect of **imperfect channel estimation** using pilot symbols.
- Study the trade-off between having multiple transmissions and the **latency**. In section 4.7, we tried to analyse this issue considering a hypothetical scenario. This can be extended to more realistic scenarios and the trade-off can be quantified in some way.
- In this era of Artificial Intelligence, it is important to study the Machine Learning techniques that can decide on optimal set of rates based on the current channel conditions and interference level. Design a neural network that classifies locations of coverage into different contours and assigns respective MCS and retransmission protocols [16] (Figure 5.1)

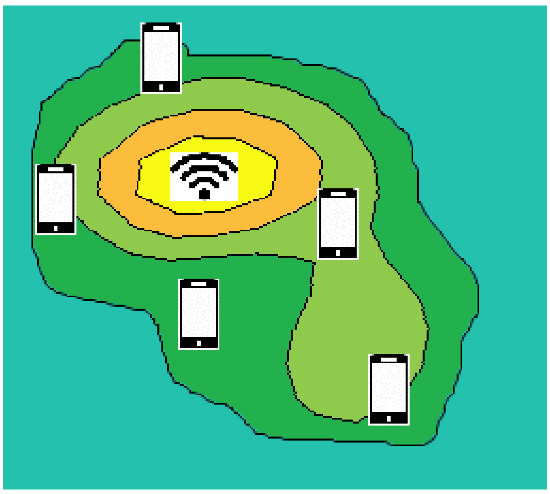

Figure 5.1: Location contours defined by Artificial Intelligence

CHAPTER 6

CONCLUSIONS

In this work, the advantages of having HARQ protocols (Incremental Redundancy (IR) in particular) over the existing ARQ scheme in WLAN 802.11 standards was analysed. It has been demonstrated via simulations that IR-HARQ can provide an SNR gain of around 3 dB over the ARQ protocols. More accurate the feedback about the channel conditions, better the IR-HARQ performance. It was observed that having an erroneous SNR feedback (variation of [-5,5] dB) can reduce the performance by a dB or so.

As the performance of IR-HARQ is significantly impacted by the puncturing scheme, it is important to have an efficient way of puncturing that minimizes the performance gap between a dedicated code and a punctured code. Since it is important to have a reasonable PER that higher layers can take care of, the throughput has to be maximised considering the PER constraint. It was observed that having a conservative PER constraint of 10^{-2} did not affect the throughput performance much, whereas the performance took a significant hit while having an aggressive constraint of 10^{-3}.

Finally, as all these benefits of IR-HARQ are coming at a cost of additional latency, it is important analyse and quantify the trade-off between throughput and latency. We studied that choosing the maximum number of transmissions dynamically, based on the number of active STAs gave a 7% increase in throughput as compared to fixing the maximum number of transmissions irrespective of the number of STAs.

CHAPTER 7

APPENDICES

7.1 Log-Likelihood Ratio (LLR) calculations for Higher Modulation Schemes in Rayleigh Fading

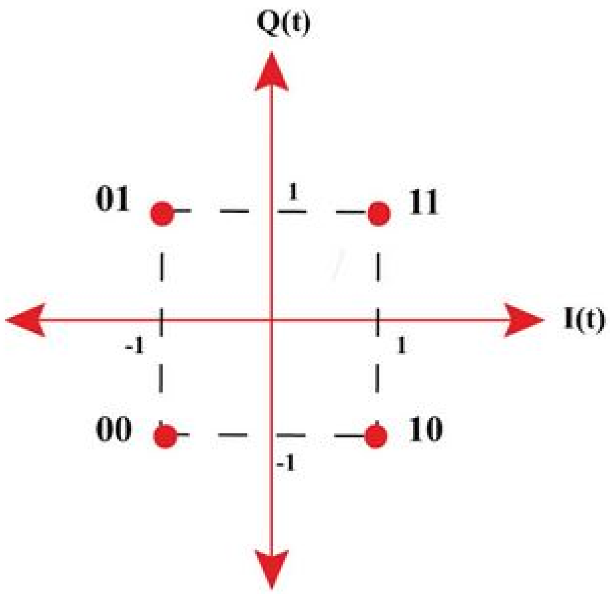

Figure 7.1: QPSK Constellation

Consider QPSK modulation.Let the received symbol be $r_x + jr_y$. In an AWGN channel, LLR for the MSB is given as follows

$$f_{AWGN}\left(r_x, r_y, \sigma^2\right) = \frac{P\left(r|b_1=0\right)}{P\left(r|b_1=1\right)} = \frac{exp\left(-\frac{(r_x+1)^2+(r_y-1)^2}{2\sigma^2}\right) + exp\left(-\frac{(r_x+1)^2+(r_y+1)^2}{2\sigma^2}\right)}{exp\left(-\frac{(r_x-1)^2+(r_y-1)^2}{2\sigma^2}\right) + exp\left(-\frac{(r_x-1)^2+(r_y+1)^2}{2\sigma^2}\right)} \tag{7.1}$$

In Rayleigh fading channel, LLR for the MSB is given as follows

$$f_{Rayleigh}\left(r_x, r_y, \sigma^2\right) = \frac{P\left(r|b_1=0\right)}{P\left(r|b_1=1\right)} = \frac{exp\left(-\frac{(r_x+h)^2+(r_y-h)^2}{2\sigma^2}\right) + exp\left(-\frac{(r_x+h)^2+(r_y+h)^2}{2\sigma^2}\right)}{exp\left(-\frac{(r_x-h)^2+(r_y-h)^2}{2\sigma^2}\right) + exp\left(-\frac{(r_x-h)^2+(r_y+h)^2}{2\sigma^2}\right)} \tag{7.2}$$

$$= \frac{exp\left(-\frac{\left(\frac{r_x}{h}+1\right)^2+\left(\frac{r_y}{h}-1\right)^2}{\frac{2\sigma^2}{h^2}}\right)+exp\left(-\frac{\left(\frac{r_x}{h}+1\right)^2+\left(\frac{r_y}{h}+1\right)^2}{\frac{2\sigma^2}{h^2}}\right)}{exp\left(-\frac{\left(\frac{r_x}{h}-1\right)^2+\left(\frac{r_y}{h}-1\right)^2}{\frac{2\sigma^2}{h^2}}\right)+exp\left(-\frac{\left(\frac{r_x}{h}-1\right)^2+\left(\frac{r_y}{h}+1\right)^2}{\frac{2\sigma^2}{h^2}}\right)} \tag{7.3}$$

Comparing eqn. 7.3 and 7.1, it can be seen that

$$f_{Rayleigh}\left(r_x, r_y, \sigma^2\right) = f_{AWGN}\left(\frac{r_x}{h}, \frac{r_y}{h}, \frac{\sigma^2}{h^2}\right) \tag{7.4}$$

7.2 802.11 WLAN channel models

WLAN 802.11ax standard defines different channel models based on the environment [14]. Channel models B and C are for residential environment, where delay spread is small. Channel models D and E are for offices, where the delay spread is relatively larger. Channel model-D was used in the simulations (Figure 4.6).

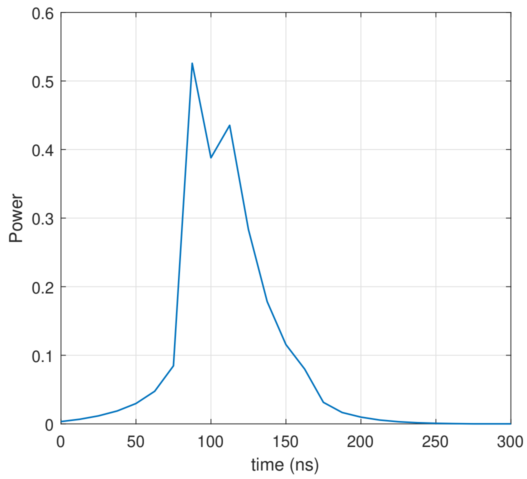

(a) Channel Model-B

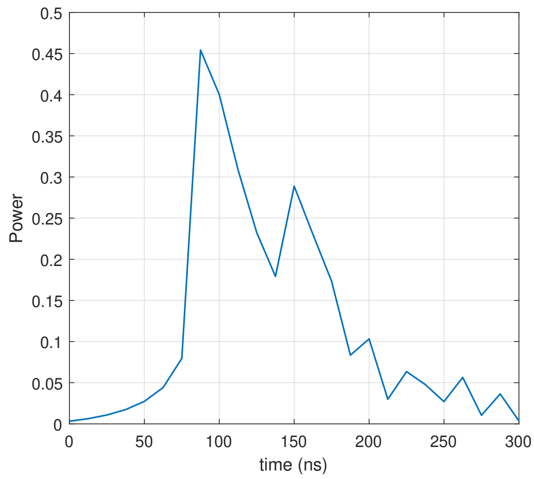

(b) Channel Model-C

Figure 7.2: WLAN TGax Channel Models for Residential Environment

7.3 K-Step Recoverable Puncturing Strategy

In all the IR-HARQ simulations described earlier, the LDPC parity bits are punctured using K-Step Recoverable (k-SR) strategy [12]

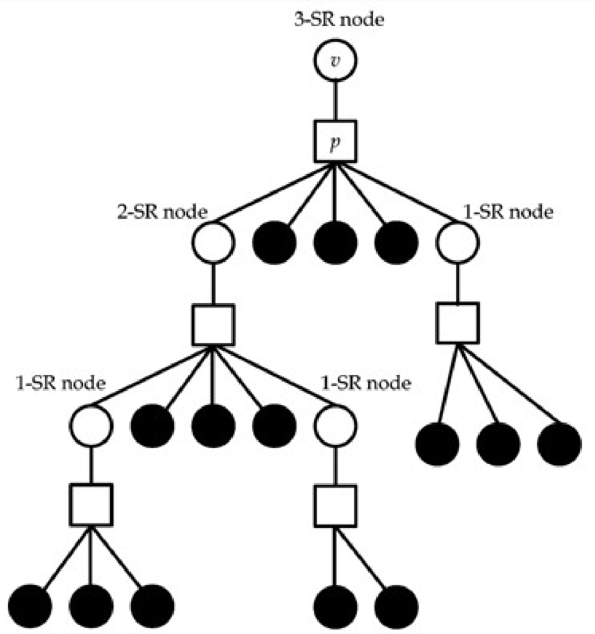

Figure 7.3: K-Step Recoverable Nodes

Consider Figure 7.3. Circled nodes are Bit nodes and square nodes are $Check$ nodes. White circled nodes are punctured bits. The first bit node in the second layer from the bottom is connected to a check node that is connected to 3 other bit nodes, all of which are not punctured. Thus, this check node passes on the LLR information to the bit node after first iteration. Hence it is labelled as 1-SR node. The punctured bit node in the next higher level is connected to two 1-SR bit nodes and 3 unpunctured nodes through a check node. These two 1-SR bit nodes, which would have received LLR information after first iteration, will pass on this information to the bit node above in the second iteration, hence the labelling 2-SR node, and so on.

$$\mathbf{H}_p=[\mathbf{H}_o|\mathbf{H}_d]=\left[\begin{array}{c|ccccc}
\mathbf{P}^{b_1} & \mathbf{I} & \mathbf{0} & \dots & \mathbf{0} & \mathbf{0} \\
\mathbf{0} & \mathbf{P}^{b_2} & \mathbf{I} & \dots & \mathbf{0} & \mathbf{0} \\
\vdots & \mathbf{0} & \mathbf{P}^{b_3} & \dots & \mathbf{0} & \mathbf{0} \\
\mathbf{P}^{p} & \vdots & \vdots & \dots & \vdots & \vdots \\
\vdots & \vdots & \vdots & \dots & \mathbf{I} & \mathbf{0} \\
\mathbf{0} & \mathbf{0} & \mathbf{0} & \dots & \mathbf{P}^{b_{m_b-1}} & \mathbf{I} \\
\mathbf{P}^{q} & \mathbf{0} & \mathbf{0} & \dots & \mathbf{0} & \mathbf{P}^{b_{m_b}}
\end{array}\right]$$

Figure 7.4: LDPC Dual-Diagonal Parity Structure in 802.11 standards

LDPC codes in WLAN 802.11 standards have a dual-diagonal parity structure as shown in Figure 7.4. 2 diagonal blocks have non-zero entries and the remaining blocks are zeros. P^{b_i} represents a circular shift of Identity matrix. Because of this structure, it can be easily seen that each bit node is connected to two adjacent bit nodes via $check$ nodes.

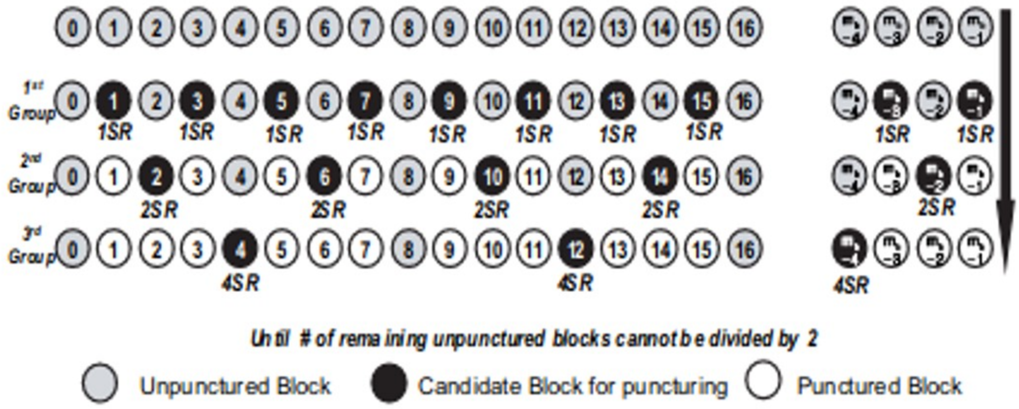

(a) Block Grouping

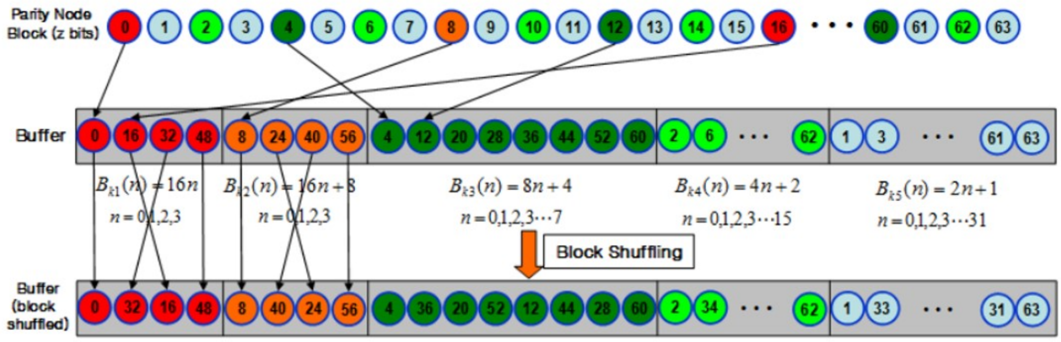

(b) Transmission Order

Figure 7.5: K-Step Recoverable Block Grouping of Parity Bits

Figure 7.5(a) defines the split of parity bits into 1-SR nodes, 2-SR nodes, 4-SR nodes and so on. As each bit node is connected to two adjacent bit nodes, alternative nodes form 1-SR group. Note that these 1-SR nodes $\{1, 3, 5, ..\}$ get LLR information from adjacent even numbered nodes after one iteration. Now, among the remaining set of nodes $\{0, 2, 4, 6, ...\}$, alternative set of nodes $\{2, 6, 10, ...\}$ form 2-SR group as they receive LLR information after 2 iterations. This process is continued until all the parity nodes are labelled.

Figure 7.5(b) defines the transmission order (reverse of puncturing order) of parity nodes based on k-SR grouping. Reliability of k-SR nodes reduces with increasing k as higher k implies more number of iterations before a reliable information is received. Hence, these nodes with low reliability have to be transmitted first followed by nodes of higher reliability. Thus, 16-SR nodes are transmitted first, followed by 8-SR nodes, 4-SR nodes, 2-SR nodes and 1-SR nodes.

7.4 Distributed Coordination Function (DCF) Analysis in 802.11 WLAN standards

Let n be the number of active STAs, W be the minimum contention window length, m be the number of transmissions upto which the contention window length keeps doubling, K be the maximum number of transmissions allowed, p be the collision probability and W_{avg} be the average contention window length.

7.4.1 Collision Probability

The contention window is initially set to W. An arbitrary packet is successfully transmitted with probability $(1-p)$, and the average backoff window of such a packet is $\frac{W-1}{2}$. If the first transmission fails, the packet is successfully transmitted on the second attempt with probability $p(1-p)$. The average backoff window in this case is $\frac{2W-1}{2}$. The backoff window, however, will only be increased until it reaches $CW_{max} = 2^m W$. Thus the overall average backoff window can be calculated as follows [17]

$$W_{avg} = \left(\frac{1-p}{1-p^{K+1}}\right)\left(\frac{W-1}{2} + p\frac{2W-1}{2} + ... + p^m\frac{2^mW-1}{2} + ... + p^K\frac{2^mW-1}{2}\right) \tag{7.5}$$

where $(1-p^{K+1})$ is the normalisation term to ensure the probability of each backoff stage follows a valid probability distribution. Based on overall average backoff window, the probability that a station attempts to transmit in an arbitrary slot is given by $\frac{1}{W_{avg}}$. The probability that during the transmission of an arbitrary station there is no other active station is $\left(1-\frac{1}{W_{avg}}\right)^{n-1}$. The collision probability p is then given as follows

$$p = 1 - \left(1 - \frac{1}{W_{avg}}\right)^{n-1} \tag{7.6}$$

Equations 7.5 and 7.6 establish a fixed point formulation between W_{avg} and p from which the collision probability p can be computed using a numerical technique.

In the Figure 4.23, as expected, with very less STAs, the collision probability is low. As the number of STAs increase, more and more collisions occur.

7.4.2 Average Packet Delay

The expected packet delay is given as follows

$$E[D] = E[X]E[slot] \tag{7.7}$$

where $E[X]$ is the average number of slots the packet spent before winning the contention for the channel and $E[slot]$ is the average length of a slot time.

The average number of slots spent is $\frac{W-1}{2}$ with probability $(1-p)$, and $\frac{2W-1}{2}$ with probability $p\,(1-p)$ and so on. Thus,

$$E[X] = \sum_{i=0}^{K} (1-p) \left(\frac{p^i - p^{K+1}}{1 - p^{K+1}} \right) \left(\frac{W_i - 1}{2} \right) \tag{7.8}$$

where p^{K+1} is subtracted from numerator and denominator to ensure a valid probaility distribution.

Let P_{tr} be the probability that at least one station (out of n) transmits in a considered slot time.

$$P_{tr} = 1 - \left(1 - \frac{1}{W_{avg}} \right)^n \tag{7.9}$$

Let P_s be the probability that a transmission occurring on the channel is successful. It is given by the probability that only one station transmits and the $n-1$ remaining stations defer, with the condition that a transmission occurs on the channel.

$$P_s = \frac{n \left(1 - \frac{1}{W_{avg}} \right)^{n-1}}{W_{avg} P_{tr}} \tag{7.10}$$

A slot can either be empty, in which case the slot time is σ, or the channel might be busy because of a successful transmission of some other node, in which case the slot time is T_s, or the channel might be busy because of a failed transmission of some other node, in which case the slot time is T_c. Weighting these different possibilities with their corresponding probabilities,

$$E[slot] = (1 - P_{tr})\,\sigma + P_{tr}P_sT_s + P_{tr}\,(1 - P_s)\,T_c \qquad (7.11)$$

Expressions from equations 7.8 and 7.11 is substituted in 7.7 to obtain the average packet delay.

7.5 Flowchart of Incremental Redundancy process

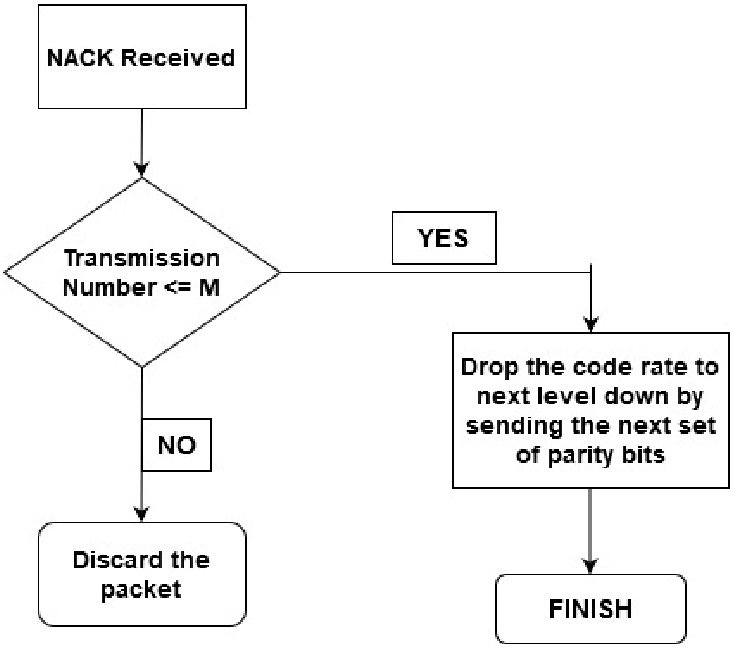

Figure 7.6: Flowchart of Incremental Redundancy process on receiving a Negative Acknowledgement

7.6 Pseudocodes of the simulations

Algorithm 1 Generate Transmit Samples

```
procedure TRANSMITTER(retx_info, modulation_order, tx_num)
    b ← Generate random bits
    b ← Attach_CRC(b)
    if retx_info.type == IR_HARQ then
        Mother_code_rate = min(retx_info.rates)
    else
        Mother_code_rate = max(retx_info.rates)

    b ← LDPC_ENCODING(b, Mother_code_rate)
    p ← PUNCTURING(b, retx_info.rates, tx_num)
    int_b ← INTERLEAVING(p)
    s ← MODULATION(int_b, modulation_order)
    t ← IFFT(s)
    t ← Add CP(t)
return t
```

Algorithm 2 Decode Received Samples

```
procedure RECEIVER(r, retx_info, modulation_order, SNR, tx_num)
    llr ← Zero Vector
    r ← Remove CP(r)
    s ← FFT(r)
    l ← DEMODULATION(s, modulation_order, SNR)
    l ← DEINTERLEAVING(l)
    l ← Fill punctured llr's with zeros(l)

    if retx_info.type == ARQ then
        llr ← l
    else
        llr ← llr + l

    dec_b ← LDPC_DECODING(llr)
    CRC_err ← CRC_DECODING(dec_b)

return CRC_err
```

Algorithm 3 Channel+Noise impairments

procedure CHANNEL_NOISE(t, SNR)
    $chnl \leftarrow$ Generate channel taps
    $r \leftarrow chnl(t)$
    $n \leftarrow$ NOISE($power = -SNR$ (in dB))
    $r \leftarrow r + n$

return r

Algorithm 4 Throughput simulations

procedure THRPT_SIM($pkt\_num, retx\_info, SNR\_list, modulation\_list, SNR\_mismatch$)

    $best\_throughput \leftarrow$ Empty vector

    for SNR in SNR_list **do**
        $throughput \leftarrow$ Empty vector
        for $modulation$ in $modulation\_list$ **do**
            $cur\_thrpt \leftarrow 0$
            for pkt in pkt_num **do**
                for tx_num in *retx_info.limit* **do**
                    $t \leftarrow$ TRANSMITTER($retx\_info, modulation$)
                    $r \leftarrow$ CHANNEL_NOISE(t, SNR)
                    $CRC\_err \leftarrow$ RECEIVER($r, retx\_info, modulation, SNR$)

                    if $CRC\_err == 0$ **then**
                        $State \leftarrow Success$
                        break

                if $State == Success$ **then**
                    $cur\_thrpt \leftarrow cur\_thrpt + \frac{modln\_order \times retx\_info.rates(tx\_num)}{pkt\_num}$

                $retx\_info.rates \leftarrow$ RATE_DECISION($SNR, SNR\_mismatch$)

            $throughput \leftarrow$ append($throughput, cur\_thrpt$)

        $best\_throughput \leftarrow$ append(best_throughput,max($throughput$))

Algorithm 5 Throughput simulations with PER constraints

procedure PER_CONSTR($pkt\_num, retx\_info, SNR\_list, modulation\_list, PER\_constr$)

$best\_throughput \leftarrow$ Empty vector

for SNR in SNR_list **do**
  $throughput \leftarrow$ Empty vector
  for $modulation$ in $modulation\_list$ **do**
    $cur\_thrpt \leftarrow 0$
    $PER \leftarrow 0$
    for pkt in pkt_num **do**
      for tx_num in *retx_info.limit* **do**
        $t \leftarrow$ TRANSMITTER($retx\_info, modulation$)
        $r \leftarrow$ CHANNEL_NOISE(t, SNR)
        $CRC\_err \leftarrow$ RECEIVER($r, retx\_info, modulation, SNR$)

        if $CRC\_err == 0$ **then**
          $State \leftarrow Success$
          break

      if $State == Success$ **then**
        $cur\_thrpt \leftarrow cur\_thrpt + \frac{modln\_order \times retx\_info.rates(tx\_num)}{pkt\_num}$
      else
        $PER \leftarrow PER + \frac{1}{pkt\_num}$

      $retx\_info.rates \leftarrow$ RATE_DECISION(SNR)

    if $PER \leq PER\_constr$ **then**
      $throughput \leftarrow$ append($throughput, cur\_thrpt$)
    else
      $throughput \leftarrow$ append($throughput, 0$)

  $best\_throughput \leftarrow$ append(best_throughput,max($throughput$))

REFERENCES

[1] Igor Stanojev, Osvaldo Simeone, Y. Bar-Ness, and Dong Ho Kim. Energy efficiency of non-collaborative and collaborative Hybrid-ARQ protocols. *IEEE Transactions on Wireless Communications*, 8, Jan 2009.

[2] Wozencraft J.M. and Horstein M. Digitalised communication over two-way channels. *Fourth London Symposium on Information Theory*, Sep 1960.

[3] J. P. M. Schalkwijk and T. Kailath. A coding scheme for additive noise channel with feedback—1, no bandwidth constraint. *IEEE Transactions on Wireless Communications*, 1966.

[4] V. K. N. Lau. Channel capacity and error exponents of variable rate adaptive channel coding for rayleigh fading channels. *IEEE Transactions on Wireless Communications*, Sep 1999.

[5] Erik Dahlman and Stefen Parkwall and Johan Skold. *5G NR: The Next Generation Wireless Access Technology*. Academic Press, 2018.

[6] LTE: Evolved universal terrestrial radio access (E-UTRA); multiplexing and channel coding (3GPP TS 36.212 version 14.2.0 release 14). *3GPP Technical Specication*.

[7] Mahmood Taher and Dr. Muhieddin Amer. Hybrid automatic repeat request in lte. *R.I.T. Dubai*, 2013.

[8] Shu Lin and Daniel J. Costello. *Error Control Coding*. Prentice Hall, 2004.

[9] Safwan H. Fasola and Firas S. Al-Sharbaty. The effect of harq procedure on the performance of lte system. Jul 2013.

[10] Ramesh Mantha. Hybrid automatic repeat request schemes using turbo codes and low density parity check codes. *University of Toronto*, 1999.

[11] Christopher Lott, Olgica Milenkovic, and Emina Soljanin. Hybrid arq: Theory, state of the art and future directions. *2007 IEEE Information Theory Workshop on Information Theory for Wireless Networks*, Jul 2007.

[12] Jeongseok Ha, Jaehong Kim, D. Klinc, and S.W. McLaughlin. Rate-compatible punctured low-density parity-check codes with short block lengths. *IEEE*, page 3, Jan 2006.

[13] 802.11ah-2016, Part 11: Wireless LAN Medium Access Control (MAC) and Physical Layer (PHY) Specifications. *IEEE*, pages 3293–3295, Dec 2016.

[14] L. Jianhan and P. Ron. Tgax channel model. *IEEE*, page 3, Sep 2014.

[15] Wonju Lee, Osvaldo Simeone, Joonhyuk Kang, Sundeep Rangan, and Petar Popovsk. Harq buffer management: An information-theoretic view. *IEEE Transactions on Communications*, 63:4539–4550, Nov 2015.

[16] Kyle Jamieson and Hari Balakrishnan. Ppr: Partial packet recovery for wireless networks. *ACM SIGCOMM Computer Communication Review*, 37(4), Oct 2007.

[17] P. Raptis, V. Vitsas, K. Paparrizos, P. Chatzimisios, and A.C. Boucouvalas. Packet delay distribution of the IEEE 802.11 distributed coordination function. *IEEE*, pages 2–3, June 2005.